

# UCLA

## UCLA Previously Published Works

### Title

Caenorhabditis elegans PRMT-7 and PRMT-9 Are Evolutionarily Conserved Protein Arginine Methyltransferases with Distinct Substrate Specificities

### Permalink

<https://escholarship.org/uc/item/7ph2q7tt>

### Journal

Biochemistry, 56(20)

### ISSN

0006-2960

### Authors

Hadjikyriacou, Andrea  
Clarke, Steven G

### Publication Date

2017-05-23

### DOI

10.1021/acs.biochem.7b00283

Peer reviewed



Published in final edited form as:

Biochemistry. 2017 May 23; 56(20): 2612–2626. doi:10.1021/acs.biochem.7b00283.

## Caenorhabditis elegans PRMT-7 and PRMT-9 Are Evolutionarily Conserved Protein Arginine Methyltransferases with Distinct Substrate Specificities

Andrea Hadjikyriacou and Steven G. Clarke\*

Dept. of Chemistry and Biochemistry and the Molecular Biology Institute, University of California, Los Angeles, 607 Charles E. Young Dr. E., Los Angeles, CA 90095-1569. Tel.: 310-825-8754

### Abstract

*Caenorhabditis elegans* protein arginine methyltransferases PRMT-7 and PRMT-9 are two evolutionarily conserved enzymes, with distinct orthologs in plants, invertebrates, and vertebrates. Biochemical characterization of these two enzymes reveals that they share much in common with their mammalian orthologs. *C. elegans* PRMT-7 produces only monomethyl arginine (MMA) and preferentially methylates R-X-R motifs in a broad collection of substrates, including human histone peptides and RG-rich peptides. In addition, the activity of the PRMT-7 enzyme is dependent on temperature, the presence of metal ions, and the reducing agent dithiothreitol (DTT). *C. elegans* PRMT-7 has a different substrate specificity and preference from the mammalian PRMT7, and the available X-ray crystal structures of the PRMT7 orthologs show differences in active site architecture. *C. elegans* PRMT-9, on the other hand, produces symmetric dimethylarginine (SDMA) and MMA on SFTB-2, the conserved *C. elegans* ortholog of the human RNA splicing factor SF3B2, indicating a possible role in regulation of nematode splicing. In contrast to PRMT-7, *C. elegans* PRMT-9 appears to be biochemically indistinguishable from its human ortholog.

### Graphical abstract

---

\*Corresponding Author: Dept. of Chemistry and Biochemistry and the Molecular Biology Institute, University of California, Los Angeles, 607 Charles E. Young Dr. E., Los Angeles, CA 90095-1569. Tel.: 310-825-8754; clarke@mbi.ucla.edu.

#### ACCESSION CODES

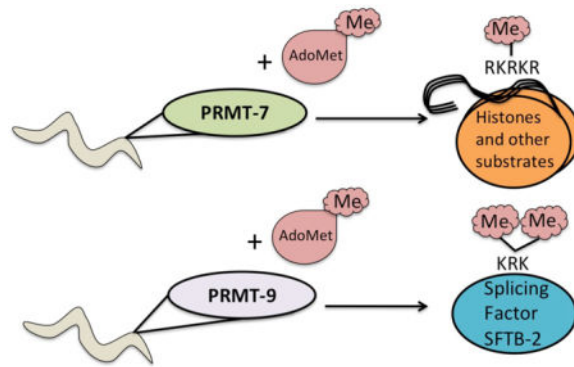
*C. elegans* PRMT-7 (UniProt ID: Q9XW42), *C. elegans* PRMT-9 (Uniprot ID: O02325), human PRMT7 (UniProt ID: Q9NVM4), human PRMT9 (UniProt ID: Q6P2P2), *C. elegans* SFTB-2 (UniProt ID: O16997), human SF3B2 (UniProt ID: Q13435) and amino acids 1–145 of human fibrillarlin (UniProt ID: P22087)

#### Author Contributions

A.H. and S.G.C. conceived the project and wrote the manuscript. A.H. performed the experiments. All authors have given approval to the final version of the manuscript.

#### Notes

The authors declare that they have no conflicts of interest with the contents of this article.



## Keywords

Protein arginine methylation; PRMT; methylation; *C. elegans*; methyltransferase; monomethylarginine; symmetric dimethylarginine

## INTRODUCTION

Protein arginine methylation is a posttranslational modification that is widely distributed in vertebrates, invertebrates, plants, and fungi<sup>1,2</sup>. Members of the mammalian protein arginine methyltransferase (PRMT) family modify arginine residues by introducing a methyl group onto the terminal guanidino groups, generating either exclusively monomethylarginine (MMA) (Type III, PRMT7), MMA and symmetric dimethylarginine (SDMA) (Type II, PRMT5 and PRMT9) or MMA and asymmetric dimethylarginine (ADMA) (Type I, PRMT1-4, -6, -8)<sup>3,4</sup>. This family of enzymes has roles in epigenetic regulation of transcription<sup>3</sup>, mRNA splicing<sup>5</sup>, DNA damage response<sup>6</sup>, carcinogenesis<sup>3,7,8</sup>, and signaling<sup>9</sup>. Many of these enzymes have multiple functions and roles, and changes in their expression have been implicated in tumorigenesis and disease<sup>3,4,7,8</sup>.

The majority of PRMTs have been well characterized and their physiological substrates have been identified. PRMT7 and PRMT9, however, have received much less attention. While PRMT9 appears to have a major role in the regulation of alternative splicing<sup>5</sup>, for PRMT7 the situation is more complex. Recent studies have shown that PRMT7 is involved in preserving satellite cell regenerative capacity<sup>10</sup>, regulation of germinal center formation<sup>11</sup>, induction of the epithelial-to-mesenchymal transition<sup>12</sup>, and bone development<sup>13</sup>, in addition to roles in cancer such as the promotion of breast cancer metastasis through MMP9 expression<sup>14</sup>. However, it has not yet been possible to connect these phenomena to the specific enzymatic action of PRMT7. In addition, there is evidence that crosstalk of PRMT7 with other PRMTs can modify the epigenetic code. For instance, the knockdown of PRMT7 in mammalian cells has been shown to decrease SDMA formation at arginine-3 in histone H2A and H4 in chromatin associated with specific genes<sup>10,15,16</sup> in spite of the fact that PRMT7 does not catalyze SDMA formation<sup>3,17,18</sup>. In addition, there is evidence for the association of increased levels of arginine-3 SDMA in histone H4 at specific genes with overexpression of PRMT7<sup>11</sup>. It thus appears that PRMT7 may function in conjunction with other PRMTs.

Due to the complexity of mammalian systems, PRMT7 from lower eukaryotes including *Trypanosoma brucei*<sup>19-22</sup> and *Caenorhabditis elegans*<sup>23,24</sup> has been studied. However, the trypanosome enzyme has preference for RG-rich proteins such as RBP16<sup>19,21,22</sup>, while mammalian PRMT7 has a preference for R-X-R motifs in basic sequence contexts such as those found in histone H2B<sup>17,18</sup>. A crystal structure is available for *C. elegans* PRMT-7 that is similar to that determined for *M. musculus* PRMT7, with both enzymes containing a single chain with two ancestrally duplicated methyltransferase domains stabilized by a zinc ion<sup>24,25</sup>. We note that while the *T. brucei* ortholog is named PRMT7, its structure is divergent from the *C. elegans* and mouse enzymes, lacking the duplicated domain characteristic of plant, invertebrate and vertebrate PRMT7 members<sup>1,2,19</sup>. A previous attempt to characterize *C. elegans* PRMT-7 (then named PRMT-2) *in vitro* was unsuccessful because it was enzymatically inactive under the conditions tested<sup>23</sup>. The authors of this same study<sup>23</sup> designated *C. elegans* PRMT-9 (then named PRMT-3) as a human PRMT7 ortholog, while more recent studies have shown it is more closely related to the human PRMT9<sup>1,26</sup>.

Given the similarity of the *C. elegans* and mouse PRMT7 enzymes, and the difficulty of determining the mechanism of PRMT7 action in vertebrates, we sought to characterize the *C. elegans* ortholog. We have now been able to show that although the *C. elegans* enzyme is similar to the previously studied mammalian enzyme in its ability to only form MMA marks<sup>17,18,27</sup>, the nematode enzyme has distinct specificity for recognizing arginine residues in peptides and proteins, suggesting distinct functions.

Mammalian PRMT9 had also been challenging to characterize. None of the previously characterized PRMT methyl-acceptors were recognized by human PRMT9<sup>26</sup>. However, it was possible to identify a complex with splicing factors SF3B2 and SF3B4, and to show that PRMT9 methylates SF3B2 to produce MMA and SDMA<sup>5,26</sup>. SF3B2 may be the only major substrate of this enzyme, and its modification appears to play a role in the regulation of alternative splicing<sup>5,26</sup>.

While *C. elegans* has no orthologs of mammalian PRMTs 2, 3, 4, 6, and 8, there is an ortholog of PRMT9<sup>1,2</sup>. In the previous study, this ortholog was shown to methylate recombinant histone H2A producing only MMA<sup>23</sup>. Thus, we were interested in characterizing this *C. elegans* PRMT-9 to establish whether or not it plays a similar function as mammalian PRMT9. We now show that *C. elegans* PRMT-9 is a type II enzyme that produces MMA and SDMA, but it also appears to be highly specific for the *C. elegans* ortholog of the SF3B2 splicing factor, SFTB-2.

## MATERIALS AND METHODS

### Bacterial Protein Expression and Purification

*C. elegans* PRMT-7 and PRMT-9 cDNA were cloned into a pGEX-6P-1 plasmids<sup>23</sup> and were a kind gift from Dr. Akiyoshi Fukamizu. The proteins were expressed in BL21 DE3 cells (Invitrogen); *C. elegans* GST-PRMT-7 and -9 enzymes were purified using the conditions described in<sup>26</sup>, but with induction for 20 h at 18 °C using 0.13 mM isopropyl D-thiogalactopyranoside (IPTG) for GST-PRMT-7 and 1 mM IPTG for 20 h at 18 °C for both GST-PRMT-9 wild type and A391H mutant. The enzymes were purified as described and

dialyzed overnight into 100 mM Tris-Cl, 100 mM NaCl, pH 7.5. *H. sapiens* GST-PRMT7<sup>18</sup>, GST-PRMT9<sup>26</sup>, and human GST-SF3B2<sup>5,26</sup> and were expressed and purified as described previously. GST-GAR was expressed using 0.4 mM IPTG for 20 h at 18 °C and purified similarly to the other proteins, but was dialyzed into 50 mM HEPES, 120 mM NaCl, 1 mM DTT, pH 8.0. The amino acid sequence for SFTB-2 (*C. elegans* SF3B2) was synthesized by GenScript, Inc. and cloned into a pGEX-6p-1 vector. GST-tagged SFTB-2 was purified similarly as human SF3B2, and dialyzed overnight into 10 mM Na<sub>2</sub>HPO<sub>4</sub>, 2 mM KH<sub>2</sub>PO<sub>4</sub>, 137 mM NaCl, 2.7 mM KCl, and 1 mM DTT (pH 7.4).

Each of these plasmids encodes the full sequence of the *Schistosoma japonicum* glutathione *S*-transferase (UniProt P08515) followed by linker regions of SDLEVLVLFQGPLGSGIP (*C. elegans* PRMT-7; SDLEVLVLFQGPLGSPEFP (*C. elegans* PRMT-9), SDLQVLFQGPL (*C. elegans* SFTB-2), SDLVPRGSST (human PRMT7), and SDLVPRGS (GST-GAR) followed by the full amino acid sequences of either *C. elegans* PRMT-7 (UniProt ID: Q9XW42), *C. elegans* PRMT-9 (UniProt ID: O02325), human PRMT7 (UniProt ID: Q9NVM4), human PRMT9 (UniProt ID: Q6P2P2), *C. elegans* SFTB-2 (UniProt ID: O16997), human SF3B2 (UniProt ID: Q13435) and amino acids 1–145 of human fibrillarin (UniProt ID: P22087), the latter of which has K2E and A145V substitutions. The GST-GAR fusion protein was previously erroneously reported to include human fibrillarin residues 1–148<sup>18,28</sup>. Purified proteins were analyzed via SDS-PAGE and quantified after using 10% trichloroacetic acid precipitation for a Lowry assay.

### Peptide synthesis

All H2B peptides used in these studies indicated in Table 1 were synthesized by GenScript, Inc. and further validated by MALDI-TOF mass spectrometry. Other peptides were gifts from their respective sources (see Table S1).

### In Vitro Methylation Reactions

Methylation reactions included 2  $\mu$ g of enzyme and potential methyl-accepting protein substrate (5  $\mu$ g) or peptide substrates at a final concentration of 12.5  $\mu$ M. Mixtures were incubated at the indicated temperatures using a buffer of 50 mM potassium HEPES, 10 mM NaCl, pH 8.2 unless otherwise indicated and 0.7  $\mu$ M *S*-adenosyl-L-[methyl-<sup>3</sup>H]methionine (<sup>3</sup>H-AdoMet, Perkin Elmer Life Sciences, 82.7 Ci/mmol, 0.55 mCi/ml in 10 mM H<sub>2</sub>SO<sub>4</sub>/EtOH (9:1, v/v) in a final reaction volume of 60  $\mu$ l. Given a counting efficiency of 50%, 1 fmol of radiolabeled methyl groups corresponds to 91 cpm.

### Amino Acid Analysis of Substrates Using High Resolution Cation Exchange Chromatography

Reactions with peptide substrates were stopped by the addition of 3  $\mu$ l of 25% trichloroacetic acid, and peptides were purified using OMIX C18 Zip-Tip pipette tips (Agilent Technologies). The reactions were then subjected to vacuum centrifugation to remove the Zip-Tip elution buffer consisting of H<sub>2</sub>O and acetonitrile (50:50). Protein substrate reactions were stopped by the addition of equal volume 25% (w/v) trichloroacetic acid followed by centrifugation to give the protein pellet. Methylated peptides and proteins were subsequently acid hydrolyzed, mixed with non-radioactive methylated arginine

derivatives, and separated and analyzed using high resolution cation exchange chromatography as described in<sup>5</sup>.

### Detection of Methylated Substrates after SDS-PAGE

Protein substrate methylation reactions were stopped by the addition of 0.2 volumes of 5× SDS sample loading buffer and run on a 12.6% polyacrylamide Tris-glycine gel. The gel was stained using Coomassie Blue, and after destaining overnight, gels were incubated in EN<sup>3</sup>HANCE (Perkin Elmer Life Sciences, catalog no. 6NE9701) autoradiography reagent, washed with water for 30 min and then vacuum dried. Dried gels were then placed in a cassette and exposed to autoradiography film (Denville Scientific, catalog no. E3012) at –80 °C for the amount of time indicated in the figure legends. Densitometry of the bands was done using ImageJ software.

## RESULTS

### PRMT7 is Widely Conserved in Vertebrates, Invertebrates, and Plants

The human PRMT7 sequence was analyzed by protein BLAST<sup>29</sup> and the representative orthologs were compiled into a phylogenetic tree (Fig. 1A). We found that the major PRMT structural motifs, including the AdoMet binding Post Motif I, the substrate binding double E loop, and the THW loop are well conserved (Fig. 1B). PRMT7 is widely distributed across vertebrates and invertebrates including mollusks, insects, tunicates, and nematodes, as well as in higher plants (Fig. 1A and <sup>1</sup>). Significantly, the *C. elegans* ortholog is 32% identical with the human enzyme over the full polypeptide length and has an expect value of  $3 \times 10^{-96}$ . Fungi appear to lack a PRMT7 ortholog, with the closest relatives having more similarity to PRMT1. Bacteria also seem to largely lack orthologs to PRMT7. The closest bacterial sequence homologs in *S. pneumoniae* and *Pseudanabaena sp.* are not mutual best hits to PRMT7, although the *R. leguminosarum* and *G. sulfurreducens* species are most closely related to PRMT7. In addition, the Type III (MMA forming) trypanosome *T. brucei* PRMT7<sup>19,21</sup> is most similar in sequence to human PRMT9 and is not a mutual best hit for human PRMT7. Importantly, *T. brucei* PRMT7 has a distinct substrate specificity from both human PRMT7 and PRMT9, preferring RG-rich proteins<sup>5,17–19,21,22,26</sup>.

The major conserved PRMT motifs are shown for selected species in Fig. 1B. While all of the enzymes have similar motifs common to all seven beta-strand methyltransferases (Motif I, Post Motif I, and Motif II), the *T. brucei* PRMT7 deviates significantly from the other proteins in the PRMT-specific double E loop and the THW loop. When compared to the human PRMT7, the *C. elegans* protein has an identical DHW sequence in the THW loop as well as an identical double E loop with the exception of the replacement of a single leucine residue with a valine residue. These results indicate that PRMT7 is evolutionarily conserved with a marked presence in vertebrates, invertebrates, and plants, but not in lower organisms.

### *C. elegans* PRMT-7 Produces Monomethyl Arginine

When we assayed the *C. elegans* PRMT-7 methyltransferase activity under conditions used in the previous biochemical study<sup>23</sup> (30 °C with an EDTA-containing buffer), we also found no activity (Fig. 2A, top left panel). However, upon lowering the incubation temperature to

one more favorable for *C. elegans* growth (25 °C), some enzymatic activity producing MMA was seen (Fig. 2A, top middle and right panels). Switching to a buffer containing no metal ion chelator, some activity was seen at 30 °C (Fig. 2A, bottom left panel) while much higher activity was seen at 25 °C (Fig. 2A, bottom middle and right panel). Previous work had demonstrated the partial loss of activity of the mammalian PRMT7 enzyme with EDTA<sup>18</sup>. A zinc ion is present in a zinc finger motif in both the mouse and the *C. elegans* PRMT7/PRMT-7 structures located some distance from the active site, suggesting that it may play a role in stabilizing an active conformation of the enzyme<sup>24,25</sup>. Thus, it appears that EDTA may inhibit the activity by extracting this zinc ion. In addition, the *C. elegans* PRMT-7 enzyme activity appears to be dependent on the presence of the reducing agent dithiothreitol (DTT), as was previously observed with the mammalian enzyme<sup>27</sup>. *In vitro* methylation reactions with two synthetic peptides containing R-X-R and similar sequences (pSmD3 and pRpl3) showed no activity at 25 °C without DTT (Fig. 2B, left panels), but showed significant MMA-producing activity when DTT was added to the reaction buffer (Fig. 2B, right panels) at 15 °C.

Based on reports that the expression level of PRMT7 can affect SDMA levels in mammalian histones<sup>11,12,15,16,30</sup>, we also asked if the active *C. elegans* PRMT-7 enzyme could catalyze dimethylation of arginine species. However, as shown in the expanded view of the amino acid analysis shown in Fig. 2A (right panels), we find no dimethylated product consistent with SDMA or ADMA is formed under conditions where 0.4% of the MMA product would have been detected. Thus, the *C. elegans* PRMT-7 produces only MMA and is thus a type III enzyme.

### **C. elegans PRMT-7 is Most Active at or Below Optimal Growth Temperatures**

In Fig. 2 we noted the enzyme was much more active at 25 °C than at 30 °C. *C. elegans* is able to grow at a variety of temperatures ranging from 12 °C (slowest growing) to 25 °C (fastest growing), with most studies done at 20 °C<sup>31</sup>. Continual incubation at temperatures higher than 25 °C leads to sterility<sup>31,32</sup>. We thus performed *in vitro* methylation reactions with *C. elegans* PRMT-7 and GST-GAR under a wider range of temperatures, from 0 °C to 42 °C (Fig. 3). After SDS-PAGE and fluorography, the methylation signal was quantified using densitometry and normalized. Fluorography revealed an activity maximum at 15 °C, with the enzyme still slightly active at the higher end of the physiological temperatures for *C. elegans* (20 and 25 °C). *In vitro* methylation reactions of human PRMT7 were performed as a comparison, and a similar but narrower dependence of activity on temperature is observed (Fig. 3). The temperature dependence of the human enzyme observed here with a maximal activity at 15 °C and little or no activity at 37 °C is similar to what was reported previously<sup>18</sup>.

### **C. elegans PRMT-7 Recognizes a Wider Variety of Substrates than Human PRMT7**

Once reaction conditions were optimized for activity, we tested a variety of protein and peptide substrates to compare the methyl-accepting activity with peptide and protein substrates including those recognized by the human PRMT7. Since both the human and mouse PRMT7 were shown to have a strong preference for R-X-R motifs flanked by basic residues in histone H2B peptides<sup>17,18</sup>, we decided to also test these peptides with the *C.*

*C. elegans* PRMT-7. Amino acid analysis showed that *C. elegans* PRMT-7 is able to methylate synthetic human histone H2B peptides containing residues 23–37 (Fig. 4A, bottom left panel). To determine whether the *C. elegans* enzyme better recognizes *C. elegans* amino acid sequences than human sequences, we performed the same experiment with the *C. elegans* histone H2B (20–34) peptide. Surprisingly, we found that the *C. elegans* enzyme recognized the human peptide better than the *C. elegans* peptide (Fig. 4A, bottom). We compared this activity to that of the human PRMT7 with the human peptide and the *C. elegans* peptide (Fig. 4A top panel) and found that the human enzyme did not methylate the *C. elegans* H2B peptide sequence. These results suggest that, at least *in vitro*, histone H2B may not be a major substrate of PRMT-7 in *C. elegans*.

Since the *C. elegans* PRMT-7 was able to methylate the human histone H2B peptide, we then tested our collection of single R-to-K mutants of this peptide (Fig. 4B). When reacted with the wild type H2B peptide, we see similar results as in panel 4A, but the removal of a single arginine in the peptide decreased the activity greatly (Fig. 4B, bottom panels). The histone H2B R29K peptide reduced methylation counts to a level about 40%, of that of the wild type peptide sequence. The R31K and R33K mutant peptides further decreased the activity to about 10% and 22% respectively, signifying the importance of arginine residues in a sequential R-X-R motif. Since our data showed that PRMT-7 prefers an R-X-R motif in histone H2B, we tested another synthetic peptide containing an R-X-R sequence, where X is a glycine, a sequence found in many GAR-motif proteins. We tested both the *C. elegans* and human enzymes with this RGR-1 peptide at 25 °C and 15 °C, and found that the *C. elegans* enzyme weakly methylated this peptide at both temperatures (Fig. 4C, top row), while the human PRMT7 enzyme showed much less activity (Fig. 4C, bottom row), indicating a slightly broader specificity for the *C. elegans* enzyme.

Once we saw the differences in substrate specificity of the *C. elegans* PRMT-7 enzyme when compared to the previously characterized human enzyme, we tested it against another panel of synthetic peptides with various sequences containing pairs of arginine residues in R-X-R motifs as well as single arginine sequences. Upon incubation with synthetic histone H4 peptides (residues 1–21 wild type; 1–21 R3K; 1–16; 14–22), we saw greatly reduced activity when the R-X-R sequence at the C-terminus of the peptide was removed (Fig. 5A). This peptide contained the sequence of the *C. elegans* histone, one identical to that of the human. Histone H4 (1–21) R3K peptide gave just a slight decrease in methylation activity (20% decrease, Fig. 5A, top right panel), but removal of the last 5 residues in the peptide in the residues 1–16 peptide caused an almost 70% drop in activity (Fig. 5A, bottom left panel). This signified that the PRMT-7 enzyme primarily methylates the R-X-R sequence, but could also recognize and methylate a single arginine. Reacting the enzyme with a small peptide containing only the R-X-R sequence of H4 (14–22) yielded almost no activity, indicating there might be a secondary site of contact and binding for the peptide to be correctly situated in the active site (Fig. 5A, bottom right panel).

Other peptides containing R-G-R and peptides containing a single arginine residue were reacted with the *C. elegans* enzyme (Fig. 5B). In a longer peptide sequence containing two pairs of R-G-R sequences (pSmD3; Fig. 5B, top left panel), we saw very high methylation activity. In a reaction with pRpl3 peptide (Fig. 5B, top middle panel) that contains three



more widely spaced arginine residues, we see an activity that is almost double that of that seen with the RGR-1 peptide (Fig. 5B, bottom right panel). *C. elegans* PRMT-7 was not able to methylate smaller peptides, such as pR1 (containing only one R flanked by G) or a peptide containing the first 7 residues from histone H3 (Fig. 5B, bottom panels).

We then tested full-length histones as substrates of both the human and *C. elegans* PRMT7 enzymes. We methylated recombinant human histone proteins at either 15 °C or 25 °C, and separated the polypeptides on SDS-PAGE. At both temperatures, we found that the *C. elegans* PRMT-7 enzyme was active in methylating histones H2A, H2B, and H3, but only weakly methylated H4 (Fig. 6). This was a surprising result since the enzyme could methylate H4 peptides (Fig. 5A). We note that the sequence of histone H4 in humans and *C. elegans* is identical with the exception of one residue in the central domain. Human PRMT7, on the other hand, was very specific for histone H2B as noted previously<sup>17</sup>, indicating a distinct difference in substrate specificity between the two enzymes.

### Crystal Structures of PRMT7 Orthologs Unveil a Distinct Pocket in the Active Site Potentially Contributing to Substrate Specificity

Although the characterized mammalian, trypanosome, and *C. elegans* PRMT7 homologs all produce MMA, there are significant differences in their substrate specificity (this study,<sup>18,22</sup>). We therefore examined the active site architecture of the available PRMT7 crystal structures of each of these enzymes. The substrate arginine residue is generally bound between the two glutamate residues in the double E loop<sup>3,4,22</sup>. The distance between the side chain carboxyls of the two glutamates in the double E loop is relatively similar (7.6 Å and 7.2 Å) in the *C. elegans* and *T. brucei* enzymes, compared to a greater distance (8.7 Å) in the *M. musculus* enzyme (Fig. 7). In addition, in PRMT7 from *C. elegans* and *T. brucei*, there is a phenylalanine residue that protrudes into the active site (F33 and F71) and may limit the size of a methyl-accepting sequence. The distance between the side chain carboxyl carbon of the second glutamate residue of the double E loop and the closest side chain carbon of the phenylalanine residue is 5.2 and 5.8 Å in *C. elegans* and *T. brucei* respectively (Fig. 7A and 7B). However, the corresponding residue in *M. musculus* PRMT7 is a serine residue whose beta carbon is much further (8.5 Å) from the glutamate residue (Fig. 7C), potentially creating a pocket that could accommodate arginine residues flanked by residues with bulkier side chains such as lysine residues. We also note that the two acidic residues in the interior of the double E loop (colored in purple in Fig. 7) are more exposed to the surface in *M. musculus* (Fig. 7C) than the corresponding residues in the *C. elegans* or *T. brucei* enzymes. These results provide insight into the broader substrate specificity of the non-mammalian PRMTs.

### *C. elegans* PRMT-9 Enzyme Methylates RNA Splicing Factor SFTB-2/SF3B2 and Forms SDMA

We previously showed a phylogenetic tree demonstrating a *C. elegans* ortholog of PRMT9 present in higher organisms<sup>26</sup>; this ortholog was originally named PRMT-3 but is now designated PRMT-9<sup>1,23,26</sup>. In addition, *C. elegans* also contains an ortholog of mammalian splicing factor SF3B2, now designated SFTB-2. SF3B2 is the only identified substrate of mammalian PRMT9<sup>5,26</sup>. To determine if the *C. elegans* PRMT-9 plays a similar

physiological role by methylating SFTB-2, we analyzed the products of both human and *C. elegans* PRMT9 enzymes with the methylatable fragment F3 of both splicing factors, corresponding to human residues 401–550 and *C. elegans* residues 99–248 (Fig. 8A). When the *C. elegans* enzyme was incubated with the *C. elegans* SFTB-2 and mammalian SF3B2 fragments, we detected both MMA and SDMA formation (Fig. 8A, top panels). In a control experiment, we also detected MMA and SDMA formation with the human enzyme and substrate (Fig. 8A, bottom right panel). However, when we reacted the human enzyme with the *C. elegans* SFTB-2 polypeptide, we only found a small MMA peak; no SDMA was detected (Fig. 8A, bottom left panel). SF3B2 and SFTB-2 are similar in sequence in the conserved region surrounding the R508 methylation site in the human protein<sup>5,26</sup> but diverge in the N-terminal region (Fig. 8B).

To ask if the *C. elegans* enzyme was specific for the same site, we reacted *C. elegans* PRMT-9 with the wild type and R508K mutant of the human SF3B2 fragment (Fig. 9). We observed that methylation was abolished in the fragment with the R508K mutation (Fig. 10B, top and bottom right panels), as compared to the wild type SF3B2 fragment (Fig. 10 A, top and bottom left panels), suggesting that the mammalian and *C. elegans* enzymes share the same strict specificity for this arginine residue in the splicing factor.

### C. elegans PRMT-9 Does Not Recognize non-SFTB-2/SF3B2 Substrates

Since most PRMTs recognize a variety of substrates, we tested multiple known substrates with the *C. elegans* enzyme, including GST-GAR, RNA binding protein Rbp16, and recombinant histones H2A and H2B (Fig. 10). Amino acid analysis of reactions using the same conditions as described in Takahashi et al.<sup>23</sup>, the first study to detect MMA activity with this PRMT-9 enzyme, showed that it did not appreciably methylate these substrates (Fig. 10A, top right panel). We did, however, observe a very small MMA activity upon the methylation of recombinant histone H2A, consistent with the previous result<sup>23</sup>. We also analyzed these reaction mixtures, along with corresponding mixtures with the human PRMT9 enzyme, using SDS-PAGE fluorography, and observed that both PRMT9 enzymes only methylated their corresponding SF3B2 substrate fragments (Fig. 10B).

### Temperature Dependence of *C. elegans* PRMT-9

We next compared the activity at various temperatures of both the human and nematode PRMT9 enzymes with the human SF3B2 substrate using SDS-PAGE fluorographic analysis (Fig. 11). We found that the *C. elegans* enzyme is active at the physiological growing temperatures for the nematode<sup>31</sup>, while the human enzyme is most active at the body's expected physiological temperature of 37 °C<sup>26</sup>. These PRMT9 enzymes are active over a wider range of temperatures than the PRMT7 enzymes analyzed in Fig. 3.

### THW Loop Residues are Responsible for the SDMA-forming Ability of *C. elegans* PRMT-9

The central residue in the conserved THW loop has been shown to play a role in the formation of MMA and SDMA in *T. brucei* PRMT7 and in human PRMT9 (23). Specifically, mutating the central cysteine residue in the human PRMT9 THW motif to histidine greatly enhanced the ability of the enzyme to form MMA and decreased its ability to form SDMA<sup>22</sup>. Making the same mutation in the *C. elegans* PRMT-9 enzyme, converting

the alanine residue in the central position of the THW loop to a histidine residue, resulted in the loss of SDMA formation and reduced MMA formation (Fig. 12). The inverse H300A mutation made in the *C. elegans* PRMT-7 enzyme results in the loss of activity (data not shown). Interestingly, additional DTT added to the reaction mixtures, for both the wild type and A391H mutant enzymes (blue line in all panels) enhanced the formation of MMA but did not affect the formation of SDMA (Fig. 12).

## DISCUSSION

While many different physiological roles have been described for PRMT7<sup>10–16,30</sup>, endogenous *in vivo* substrate(s) have yet to be identified. PRMT7 is widely distributed across vertebrates, invertebrates, and plants. Fungi such as *S. cerevisiae* and *E. pusillum* do not contain a PRMT7 ortholog, as their top BLAST hits match well with the major PRMT1 ortholog (Fig. 1). Other studies have not found corresponding orthologs in *S. cerevisiae* and *S. pombe*<sup>1</sup>. What was most surprising is our identification of potential bacterial PRMT7 orthologs from *R. leguminosarum* and *G. sulfurreducens* that were mutual best hits to human PRMT7. Methylation of arginine residues has never been observed in bacteria, and no PRMT genes have been previously reported in bacteria. These prospective bacterial orthologs lack an apparent THW loop and do not contain the ancestrally duplicated C-terminal domain, much like the *T. brucei* ortholog of PRMT7. *G. sulfurreducens* does contain the characteristic TPR motifs of human PRMT9, yet the closest human hit when analyzed with protein BLAST is PRMT7. Further work needs to be done to confirm if these potential enzymes actually methylate arginine residues. Presumably, the retention of PRMT7 in higher organisms reflects its specific cellular roles, including the limitation of its activity to monomethylation, its substrate specificity, and its potential for regulation and crosstalk with other modifying enzymes.

Optimizing reaction conditions for the *C. elegans* PRMT-7 enzyme, such as lowering the reaction temperature, removing metal ion chelators and adding reducing agents such as DTT, proved to be essential for determining its substrate preference and methylation activity. While the optimal temperature for the activity of *C. elegans* PRMT-7 falls clearly in the physiological range of this organism, the human PRMT7 enzyme also demonstrates a similar temperature preference range where it is much more active than it is at 37 °C. This is an unusual property for a human enzyme, and may be important in its activity in regions of localized hypothermia such as in lung tissue exposed to cold air or in the extremities. It would be interesting to correlate the function of PRMT7 with the expression of cold-inducible RNA-binding proteins CIRP and RBM3, both of which are known to be methylated at arginine residues<sup>33</sup>. Alternatively, the small amount of activity of human PRMT7 at 37 °C may be sufficient for its function or there may be other proteins or small molecules present in human cells that allow for enhanced activity at normal body temperature.

We show here that *C. elegans* PRMT-7 methylates human histone H2B peptides, prime *in vitro* substrates for the human PRMT7 enzyme, but less methylation of the corresponding *C. elegans* H2B peptide was seen (Fig. 4A). This result suggests that histone H2B may not be a major physiological substrate for the *C. elegans* PRMT-7. It has been shown in proteomic

studies that there is divergence in conservation of methylation sites across various organisms<sup>34</sup>, indicating the methylation sites can differ across different species and organisms.

Our results also indicate the importance of multiple arginine residues in an R-X-R motif for recognition by both *C. elegans* PRMT-7 and human PRMT7. However, the *C. elegans* enzyme does not appear to have a strong preference for adjacent basic residues and methylated substrates with adjacent glycine residues such as pSmD3. Peptides with single arginine residues were generally not substrates, but a histone H4 1–16 peptide containing a single arginine residue was weakly methylated by *C. elegans* PRMT-7. It appears that the length of the peptide, the positioning of arginine residues, as well as the nature of adjacent and distant residues play a role in substrate specificity.

Comparison of the activity of the human and *C. elegans* PRMT7s on intact human recombinant histones confirms the specificity of the human enzyme for H2B<sup>17</sup>. However, we observe here that the *C. elegans* PRMT-7 methylates all of the histone proteins, with the exception of only weakly methylating histone H4 (Fig. 6). This broader substrate methylation leads us to believe that its physiological substrates, while not identified yet, could potentially be different from and more numerous than those of its mammalian ortholog.

To further probe the substrate specificity of these enzymes, we examined the active site architectures of *C. elegans*<sup>24</sup>, *T. brucei*<sup>20</sup>, and *M. musculus* PRMT7<sup>25</sup>. Surface modeling of their crystal structures reveals differences that may relate to their activities. As discussed in the “Results” section, the distances between the two terminal glutamates in the double E loop were closer together in the *C. elegans* and *T. brucei* structures, compared to the corresponding residues in the mouse structure. In addition, there are differences in residues, in particular a phenylalanine (*C. elegans* or *T. brucei*) or serine (mouse) residue that comes in contact with the second glutamate of the double E loop. These structural differences may explain why we see such distinct substrate specificity among the various orthologs of PRMT7, indicating that the enzyme may have evolved to have different functions and substrates among different organisms. Further work needs to be done to confirm the importance of these residues in conferring substrate specificity.

*C. elegans* also has a PRMT-9 ortholog that has been conserved from invertebrates to mammals with a potentially similar physiological function. We show here that the *C. elegans* PRMT-9 enzyme produces SDMA and MMA on the splicing factor SF3B2 ortholog in *C. elegans*, SFTB-2. Additionally, we found that the enzyme methylates the same R508 residue on SF3B2 as the human enzyme, suggesting that PRMT-9 may also play a regulatory role in nematode alternative RNA splicing. It will now be important to directly examine at the effect of methylation of SFTB-2 on the regulation of splicing in *C. elegans*, a process that has been shown to bear similarities to human splicing mechanisms<sup>35</sup>.

## Supplementary Material

Refer to Web version on PubMed Central for supplementary material.

## Acknowledgments

The authors would like to thank Alexander Patananan (UCLA) for his advice on *C. elegans* biology and to Akiyoshi Fukamizu (University of Tsukuba, Japan) for providing the cDNA clones of *C. elegans* GST-PRMT-7 and GST-PRMT-9. The authors also thank Adam Frankel (University of British Columbia) for the R1 peptide, and Mark T. Bedford (MD Anderson Cancer Center) for the GST-SF3B2 plasmid. The authors also would like to thank members of the Clarke laboratory, in particular Jonathan Lowenson, Kanishk Jain, and Rebecca Warmack for useful comments on the manuscript.

### Funding Sources

This work was supported, in whole or in part, by National Institutes of Health Grants GM026020 (to S. G. C.) and GM007185, a Ruth L. Kirschstein National Research Service Award (to A. H.), funds from the Elizabeth and Thomas Plott Chair in Gerontology of the UCLA Longevity Center (to S. G. C.), funds from a UCLA Dissertation Year Fellowship (to A. H.), and a UCLA Faculty Research Award (to S. G. C.).

## ABBREVIATIONS

<b>PRMT</b>	protein arginine methyltransferase
<b>MMA</b>	$\omega$ - $N^G$ -monomethylarginine
<b>ADMA</b>	$\omega$ - $N^G, N^G$ -asymmetric dimethylarginine
<b>SDMA</b>	$\omega$ - $N^G, N^G$ -symmetric dimethylarginine
<b>AdoMet</b>	<i>S</i> -adenosyl-L-methionine
<b>[methyl-<sup>3</sup>H]AdoMet</b>	<i>S</i> -adenosyl-[methyl- <sup>3</sup> H]-L-methionine
<b>GAR</b>	glycine- and arginine-rich domain of human fibrillarlin

## References

1. Wang Y, Wang J, Chen C, Chen Y, Li C. A novel BLAST-Based Relative Distance (BBRD) method can effectively group members of protein arginine methyltransferases and suggest their evolutionary relationship. *Mol Phylogenet Evol.* 2015; 84:101–111. [PubMed: 25576770]
2. Wang YC, Li C. Evolutionarily conserved protein arginine methyltransferases in non-mammalian animal systems. *FEBS J.* 2012; 279:932–945. [PubMed: 22251447]
3. Fuhrmann J, Clancy KW, Thompson PR. Chemical biology of protein arginine modifications in epigenetic regulation. *Chem Rev.* 2015; 115:5413–5461. [PubMed: 25970731]
4. Bedford MT, Clarke SG. Protein arginine methylation in mammals : Who, what, and why. *Mol Cell.* 2009; 33:1–13. [PubMed: 19150423]
5. Yang Y, Hadjikyriacou A, Xia Z, Gayatri S, Kim D, Zurita-Lopez C, Kelly R, Guo A, Li W, Clarke SG, Bedford MT. PRMT9 is a Type II methyltransferase that methylates the splicing factor SAP145. *Nat Commun.* 2015; 6:6428. [PubMed: 25737013]
6. Auclair Y, Richard S. The role of arginine methylation in the DNA damage response. *DNA Repair (Amst).* 2013; 12:459–465. [PubMed: 23684798]
7. Yang Y, Bedford MT. Protein arginine methyltransferases and cancer. *Nat Rev Cancer.* 2013; 13:37–50. [PubMed: 23235912]
8. Baldwin RM, Morettin A, Côté J. Role of PRMTs in cancer: Could minor isoforms be leaving a mark? *World J Biol Chem.* 2014; 5:115–29. [PubMed: 24921003]
9. Likhite N, Jackson CA, Liang M, Krzyzanowski MC, Lei P, Wood JF, Birkaya B, Michaels KL, Andreadis ST, Clark SD, Yu MC, Ferkey DM. The protein arginine methyltransferase PRMT5 promotes D2-like dopamine receptor signaling. *Sci Signal.* 2015; 8:1–10.

10. Blanc RS, Vogel G, Chen T, Crist C, Richard S. PRMT7 preserves satellite cell regenerative capacity. *Cell Rep.* 2016; 14:1528–1539. [PubMed: 26854227]
11. Ying Z, Mei M, Zhang P, Liu C, He H, Gao F, Bao S. Histone arginine methylation by PRMT7 controls germinal center formation via regulating Bcl6 transcription. *J Immunol.* 2015; 195:1538–47. [PubMed: 26179907]
12. Yao R, Jiang H, Ma Y, Wang L, Wang L, Du J, Hou P, Gao Y, Zhao L, Wang G, Zhang Y, Liu DX, Huang B, Lu J. PRMT7 induces epithelial-to-mesenchymal transition and promotes metastasis in breast cancer. *Cancer Res.* 2014; 74:5656–5667. [PubMed: 25136067]
13. Kernohan KD, McBride A, Xi Y, Marin N, Schwartzentruber J, Dymment DA, Majewski J, Blaser S, Care4Rare Canada Consortium, Boycott KM, Chitaya D. Loss of the arginine methyltransferase PRMT7 causes syndromic intellectual disability with microcephaly and brachydactyly. *Clin Genet.* 2017; 91:708–716. [PubMed: 27718516]
14. Baldwin RM, Haghandish N, Daneshmand M, Paris G, Falls TJ, Bell JC, Islam S, Côté J. Protein arginine methyltransferase 7 promotes breast cancer cell invasion through the induction of MMP9 expression. *Oncotarget.* 2014; 6:3013–3032.
15. Karkhanis V, Wang L, Tae S, Hu YJ, Imbalzano AN, Sif S. Protein arginine methyltransferase 7 regulates cellular response to DNA damage by methylating promoter histones H2A and H4 of the polymerase  $\delta$  catalytic subunit gene, POLD1. *J Biol Chem.* 2012; 287:29801–29814. [PubMed: 22761421]
16. Dhar SS, Lee SH, Kan PY, Voigt P, Ma L, Shi X, Reinberg D, Lee MG. Trans-tail regulation of MLL4-catalyzed H3K4 methylation by H4R3 symmetric dimethylation is mediated by a tandem PHD of MLL4. *Genes Dev.* 2012; 26:2749–2762. [PubMed: 23249737]
17. Feng Y, Maity R, Whitelegge JP, Hadjikyriacou A, Li Z, Zurita-Lopez C, Al-Hadid Q, Clark AT, Bedford MT, Masson JY, Clarke SG. Mammalian protein arginine methyltransferase 7 (PRMT7) specifically targets RXR sites in lysine- and arginine-rich regions. *J Biol Chem.* 2013; 288:37010–37025. [PubMed: 24247247]
18. Feng Y, Hadjikyriacou A, Clarke SG. Substrate specificity of human protein arginine methyltransferase 7 (PRMT7) - The importance of acidic residues in the double E loop. *J Biol Chem.* 2014; 289:32604–32616. [PubMed: 25294873]
19. Fisk JC, Sayegh J, Zurita-Lopez C, Menon S, Presnyak V, Clarke SG, Read LK. A type III protein arginine methyltransferase from the protozoan parasite *Trypanosoma brucei*. *J Biol Chem.* 2009; 284:11590–11600. [PubMed: 19254949]
20. Wang C, Zhu Y, Caceres TB, Liu L, Peng J, Wang J, Chen J, Chen X, Zhang Z, Zuo X, Gong Q, Teng M, Hevel JM, Wu J, Shi Y. Structural determinants for the strict monomethylation activity by *Trypanosoma brucei* protein arginine methyltransferase 7. *Structure.* 2014; 22:756–768. [PubMed: 24726341]
21. Debler EW, Jain K, Warmack RA, Feng Y, Clarke SG, Blobel G. A glutamate/aspartate switch controls product specificity in a protein arginine methyltransferase. *Proc Natl Acad Sci.* 2016; 113:2068–2073. [PubMed: 26858449]
22. Jain K, Warmack RA, Debler EW, Hadjikyriacou A, Stavropoulos P, Clarke SG. Protein arginine methyltransferase product specificity is mediated by distinct active-site architectures. *J Biol Chem.* 2016; 291:18299–18308. [PubMed: 27387499]
23. Takahashi Y, Daitoku H, Yokoyama A, Nakayama K, Kim JD, Fukamizu A. The *C. elegans* PRMT-3 possesses a type III protein arginine methyltransferase activity. *J Recept Signal Transduct Res.* 2011; 31:168–172. [PubMed: 21385054]
24. Hasegawa M, Toma-Fukai S, Kim JD, Fukamizu A, Shimizu T. Protein arginine methyltransferase 7 has a novel homodimer-like structure formed by tandem repeats. *FEBS Lett.* 2014; 588:1942–1948. [PubMed: 24726727]
25. Cura V, Troffer-Charlier N, Wurtz JM, Bonnefond L, Cavarelli J. Structural insight into arginine methylation by the mouse protein arginine methyltransferase 7 : a zinc finger freezes the mimic of the dimeric state into a single active site. *Acta Crystallogr Sect D.* 2014; 70:2401–2412. [PubMed: 25195753]

26. Hadjikyriacou A, Yang Y, Espejo A, Bedford MT, Clarke SG. Unique features of human protein arginine methyltransferase 9 (PRMT9) and its substrate RNA splicing factor SF3B2. *J Biol Chem.* 2015; 290:16723–16743. [PubMed: 25979344]
27. Zurita-Lopez CI, Sandberg T, Kelly R, Clarke SG. Human protein arginine methyltransferase 7 (PRMT7) is a type III enzyme forming  $\omega$ - $N^G$ -monomethylated arginine residues. *J Biol Chem.* 2012; 287:7859–7870. [PubMed: 22241471]
28. Tang J, Gary JD, Clarke S, Herschman HR. PRMT 3, a type I protein arginine *N*-methyltransferase that differs from PRMT1 in its oligomerization, subcellular localization, substrate specificity, and regulation. *J Biol Chem.* 1998; 273:16935–45. [PubMed: 9642256]
29. McWilliam H, Li W, Uludag M, Squizzato S, Park YM, Buso N, Cowley AP, Lopez R. Analysis tool web services from the EMBL-EBI. *Nucleic Acids Res.* 2013; 41:597–600.
30. Jelinic P, Stehle JC, Shaw P. The testis-specific factor CTCFL cooperates with the protein methyltransferase PRMT7 in H19 imprinting control region methylation. *PLoS Biol.* 2006; 4:1910–1922.
31. Corsi, AK., Wightman, B., Chalfie, M. A transparent window into biology: A primer on *Caenorhabditis elegans*. In: De Stasio, EA., editor. *Worm Book Genetics*. Worm Book; 2015. p. 387-407.
32. Petrella LN. Natural variants of *C. elegans* demonstrate defects in both sperm function and oogenesis at elevated temperatures. *PLoS One.* 2014; 9:1–13.
33. LLeonart ME. A new generation of proto-oncogenes: Cold-inducible RNA binding proteins. *Biochim Biophys Acta - Rev Cancer.* 2010; 1805:43–52.
34. Larsen SC, Sylvestersen KB, Mund A, Lyon D, Mullari M, Madsen MV, Daniel JA, Jensen LJ, Nielsen ML. Proteome-wide analysis of arginine monomethylation reveals widespread occurrence in human cells. *Sci Signal.* 2016; 9:1–15.
35. Gracida, X., Norris, AD., Calarco, JA. *Advances in Experimental Medicine and Biology*. Springer International Publishing Switzerland; Cambridge, MA: 2016. Regulation of tissue-specific alternative splicing: *C. elegans* as a model system; p. 229-261.
36. Gottschling H, Freese E. Tritium isotope effect on ion exchange chromatography. *Nature.* 1962; 196:829–831. [PubMed: 13949509]

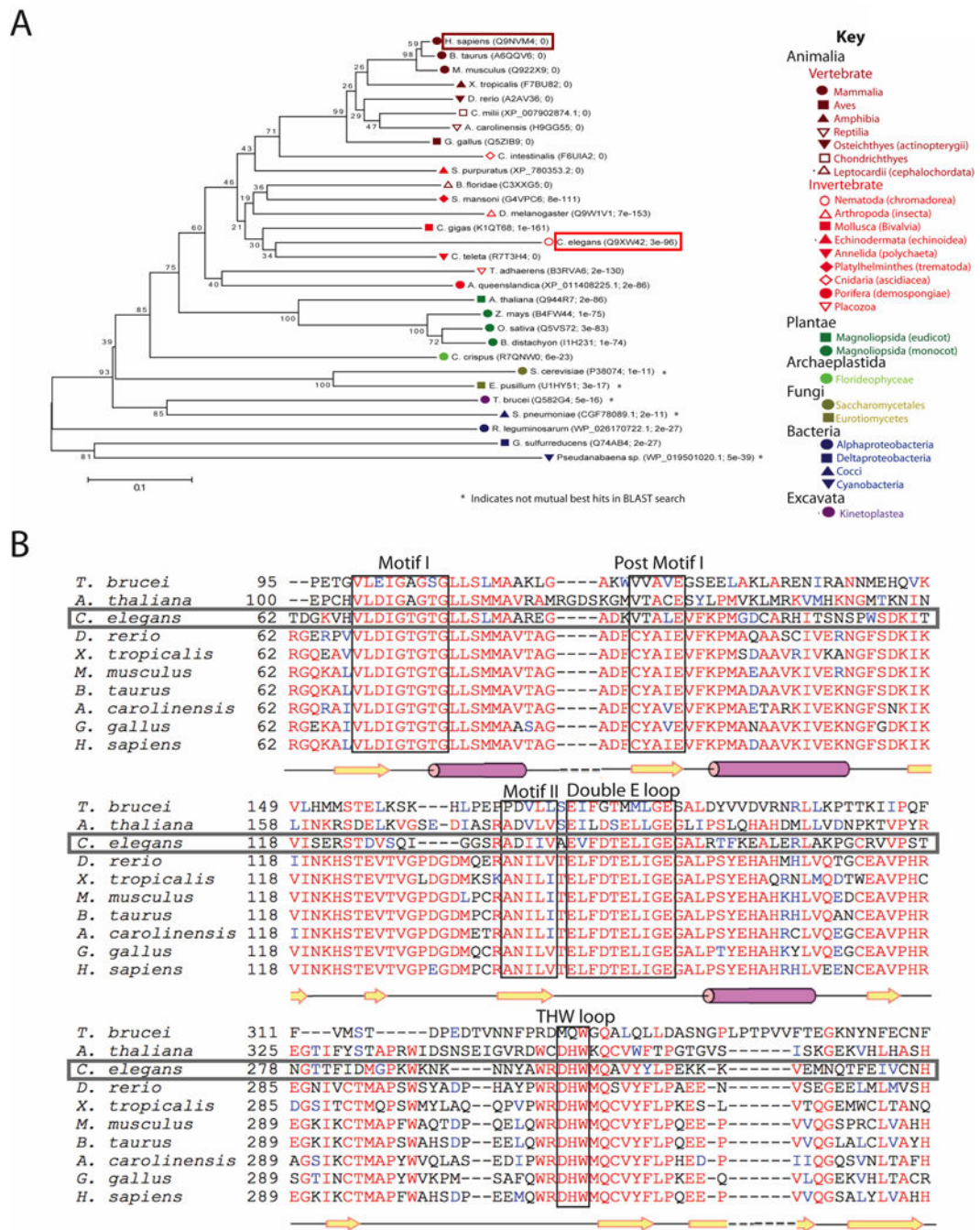


**Figure 1. Evolutionary conservation of PRMT7 across the various kingdoms of life**

A. Phylogenetic tree based on human PRMT7. UniProt IDs of representative orthologs from Animalia, Plantae, Archaeplastida, Fungi, Bacteria, and Excavata are shown with their *E* values based on a protein BLAST search against the human species<sup>29</sup>. The phylogenetic tree was constructed after amino acid sequences were aligned using MUSCLE in MEGA6 software as described in<sup>26</sup>. Each ortholog sequence was then subjected to protein BLAST against the human protein database. All proteins were mutual best hits with the exception of those species marked with an asterisk. The number shown next to each branch is the percent



of replicate trees with the same clustering in 500 bootstrap test replicates. The scale bar indicates the fraction of amino acid differences for each entry. *H. sapiens* PRMT7 is boxed in dark red, and *C. elegans* PRMT-7 is boxed in red. B. Partial sequence alignment of the major motifs in PRMT7 orthologs across vertebrates, invertebrates, plants, and excavata (*T. brucei*) using the EMBL-EBI Clustal Omega Multiple Sequence Alignment software<sup>29</sup>. The major distinguishing motifs of protein arginine methyltransferases are boxed in black, including Motif I, Post Motif I, Motif II, the Double E loop, and the THW loop. Red letters indicate identity and blue letters indicate similar amino acid properties. Secondary structure is indicated on the bottom with beta strands in yellow and alpha-helices in magenta based on the structure of the *M. musculus* PRMT7 (PDB: 4C4A,<sup>25</sup>). The *C. elegans* PRMT-7 sequence is boxed in dark gray.

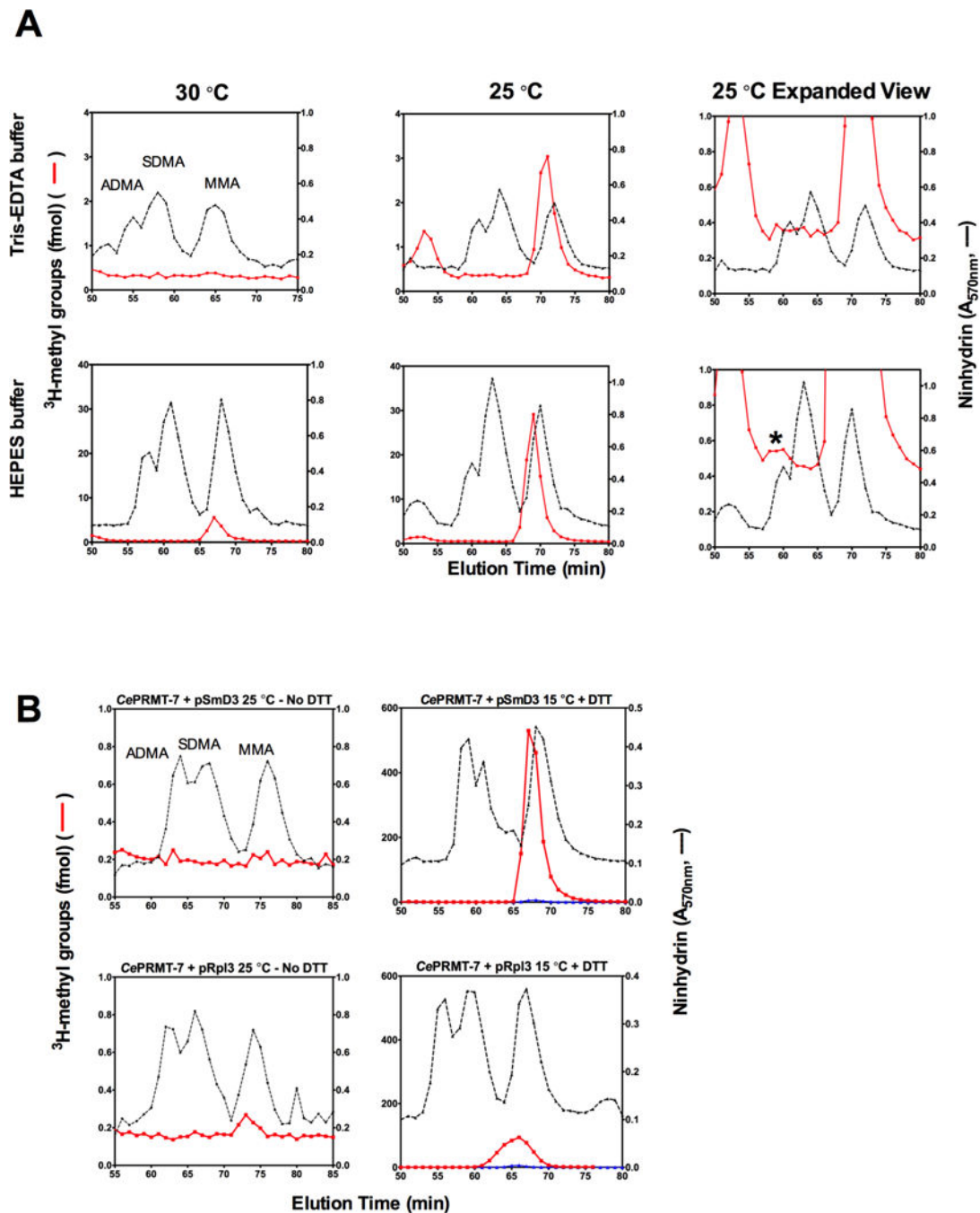


**Figure 2. *C. elegans* PRMT-7 produces MMA and its activity is temperature and metal ion dependent**

A. Amino acid analysis of <sup>3</sup>H-methylation reactions of *C. elegans* GST-PRMT-7 (2 μg) with GST-GAR (5 μg) after a 20 h reaction at 30 °C (left column) or 25 °C (middle and right columns) in either Tris-EDTA buffer (100 mM Tris-HCl, 100 mM NaCl, 2 mM EDTA, pH 8.0) (top row), or 50 mM potassium HEPES, 10 mM NaCl, pH 8.2 (bottom row) as indicated in the “Experimental Procedures” section. The final concentration of DTT in these reactions (from the GST-GAR preparation) was 0.16 mM. After trichloroacetic acid precipitation and acid hydrolysis, 1 μmol of each non-radiolabeled methylated arginine standard (ADMA,

SDMA and MMA) was added to the hydrolyzed pellet and amino acid analysis was performed as in the “Experimental Procedures” section. Dashed black lines indicate ninhydrin absorbance of the methylarginine standards with the peaks of ADMA, SDMA, and MMA identified using 50  $\mu$ l of each fraction. Red lines indicate the elution of the radiolabeled methylated amino acids from the hydrolysates of the reactions. Radioactivity from 950  $\mu$ l aliquots of each fraction is given as the average of three 5-min counting cycles using liquid scintillation counting. Radioactive methylated amino acids elute approximately 1 min before the non-radiolabeled standard due to the tritium isotope effect<sup>36</sup>. The right panels show an expanded view of the data from the middle columns at 25 °C to demonstrate that the enzyme only produces MMA under both buffer conditions. These reactions were replicated three independent times. The asterisk indicates the peak eluting prior to the position expected for <sup>3</sup>H-ADMA; this peak is not consistently observed in the replicates. B. PRMT-7 enzyme activity is dependent on presence of DTT. Enzyme was reacted with 12.5  $\mu$ M pSmD3 (top) or pRp13 (bottom) peptides at 25 °C in 50 mM potassium HEPES, 10 mM NaCl, pH 8.2 (left column), or at 15 °C in the same buffer with the addition of 1 mM DTT. Results are presented as shown in panel A; the blue line in the right hand panels indicates radioactivity for incubations where no peptide substrate was added. These reactions were replicated twice with no DTT and once with DTT.

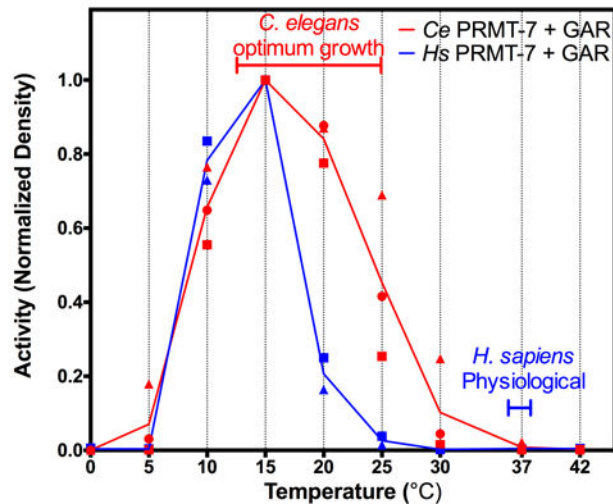
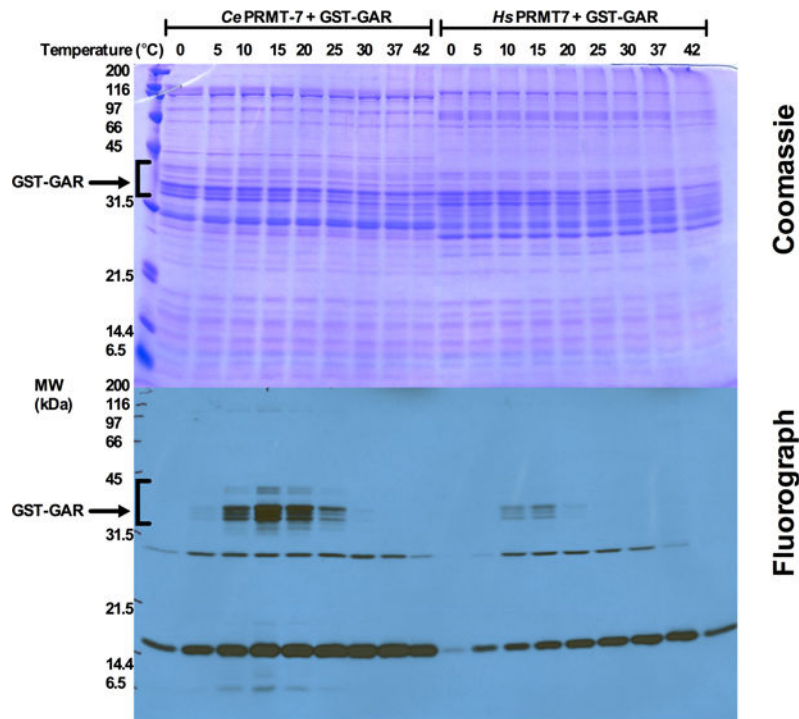


**Figure 3. PRMT-7 has a temperature dependence consistent with *C. elegans* physiology** Methylation reactions consisting of 5  $\mu\text{g}$  GST-GAR substrate and 2  $\mu\text{g}$  of enzyme (*C. elegans* GST-PRMT-7 or *H. sapiens* GST-PRMT7) were incubated for 20 h at the indicated temperatures in reaction buffer containing 50 mM potassium HEPES, 10 mM NaCl, pH 8.2, with 0.7  $\mu\text{M}$  [*methyl*- $^3\text{H}$ ]AdoMet in a final reaction volume of 60  $\mu\text{l}$ . The final concentration of DTT in these reactions (from the GST-GAR preparation) was 0.16 mM. Reactions were quenched by the addition of SDS sample loading buffer and polypeptides separated by 12.6% Tris-glycine SDS-PAGE followed by autoradiography as described in “Experimental

Procedures.” The dried gel was then exposed to Denville E3012 autoradiography film for 21 d at  $-80^{\circ}\text{C}$ . Molecular weight positions are shown from approximately  $2\ \mu\text{g}$  of unstained SDS-PAGE broad range marker (BioRad, catalog no, 161-0317). This full experiment was independently replicated and a further third replicate using only the *C. elegans* enzyme was also done. Densitometry was done using ImageJ software on scanned images of the films and quantified as relative density and normalized to the highest peak of GST-GAR radioactivity in each individual film (*C. elegans*, red symbols; human, blue symbols – different symbols used to indicate each replicate experiment). Lines are drawn for the averaged normalized values. The optimal growth temperatures for *C. elegans*<sup>31</sup> and humans are indicated. Lower bands shown on the fluorography are nonspecific and not dependent on the enzyme activity.

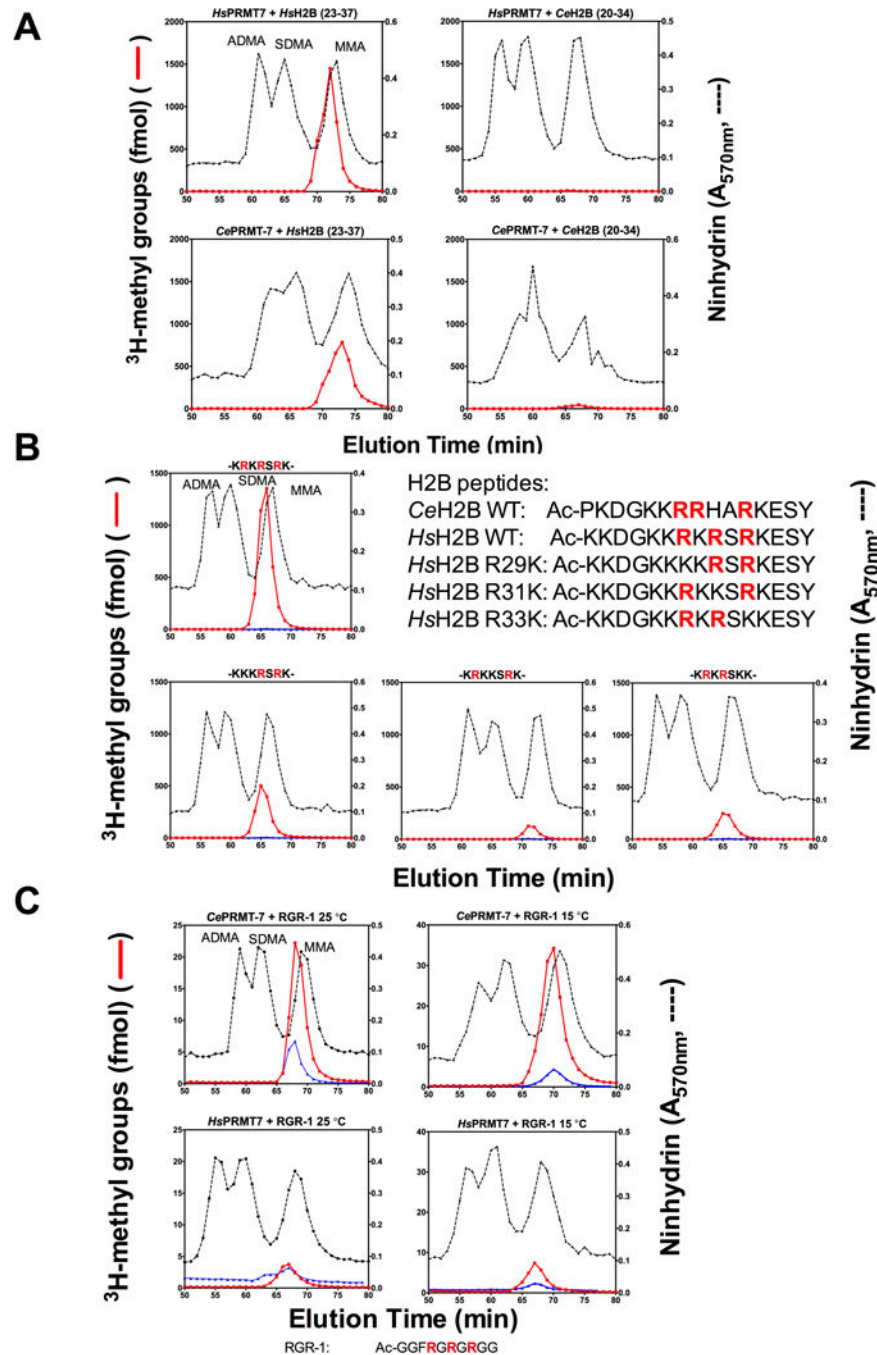


**Figure 4. *C. elegans* PRMT-7 has a similar R-X-R substrate specificity as the human PRMT7 enzyme**

A. Amino acid analysis of reactions consisting of 2  $\mu\text{g}$  of human GST-PRMT7 or *C. elegans* PRMT-7 enzymes, reacted with 12.5  $\mu\text{M}$  of synthetic human histone H2B (23–37) peptide<sup>17,18</sup> or a synthetic peptide containing the equivalent sequence from *C. elegans* histone H2B (20–34) at 15 °C as described in “Experimental Procedures,” in 50 mM potassium HEPES buffer, 10 mM NaCl, pH 8.0, containing 1 mM DTT for 20 h. Reactions were repeated three times for human histone H2B (23–37) and twice for *C. elegans* H2B (20–34) at this temperature and also replicated at 25 °C once. B. Amino acid analysis of

reactions containing 2  $\mu\text{g}$  of *C. elegans* GST-PRMT-7 enzyme reacted with 12.5  $\mu\text{M}$  synthetic human histone H2B peptides (Wild type, top; R29K, R31K and R33K bottom row) for 20 h, using the same conditions described above in panel A. These reactions were single replicates. C. Amino acid analysis of reactions containing 2  $\mu\text{g}$  of *C. elegans* or human PRMT-7/7 enzymes, reacted with 12.5  $\mu\text{M}$  of synthetic peptide RGR-1 (a sequence containing an R-X-R sequence where X = G) at 25 °C (left) or 15 °C (right), under the same reaction conditions as described in A. Reactions were replicated once and the reaction of *C. elegans* with RGR-1 was replicated an additional two times.

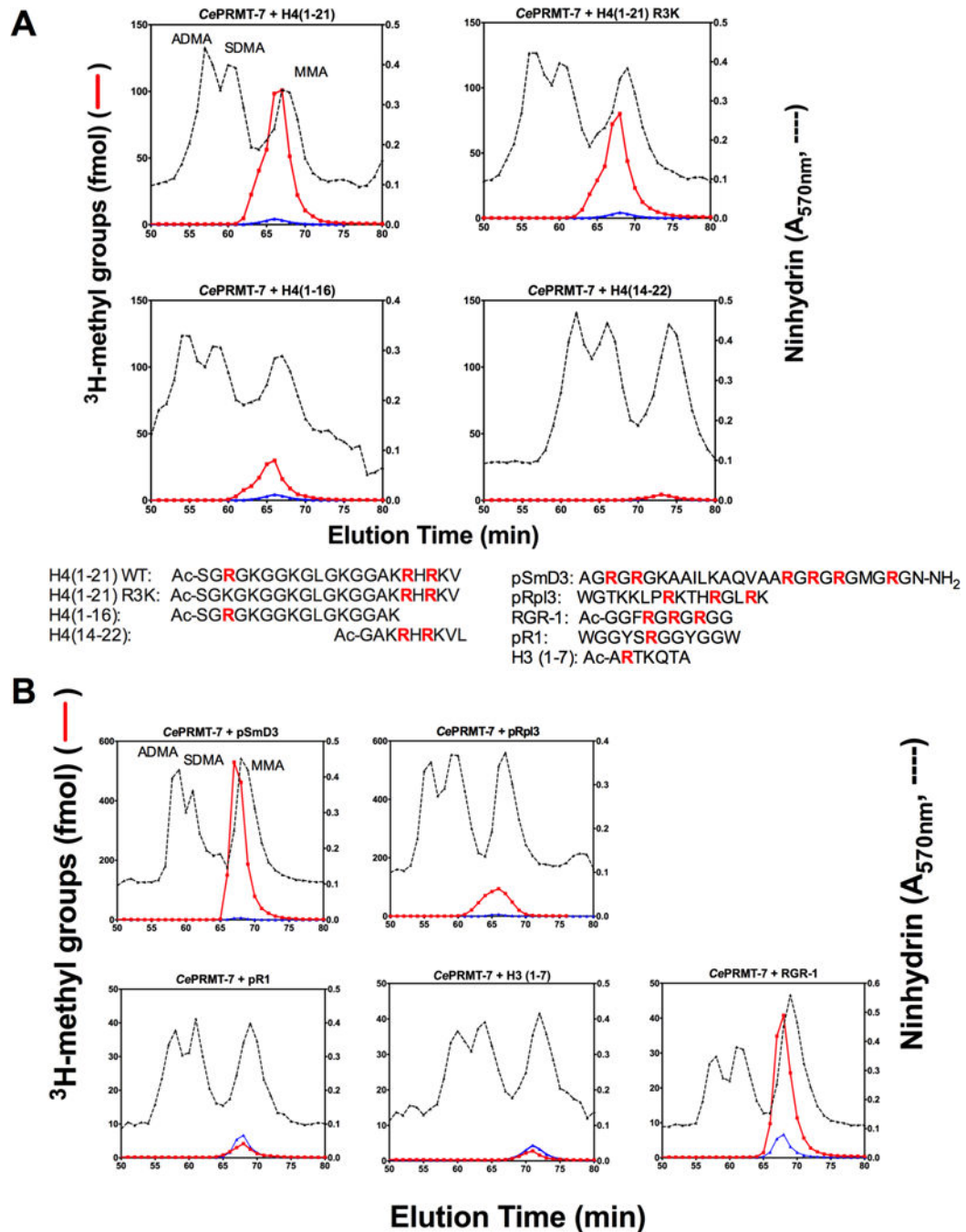


**Figure 5. *C. elegans* PRMT-7 has a preference for R-X-R motifs in various peptide substrates**  
 A. *C. elegans* PRMT-7 (2  $\mu$ g) enzyme was reacted with 12.5  $\mu$ M various synthetic human histone H4 peptides (1–21 wild type; 1–21 R3K; 1–16 wild type; and 14–22) at 15 °C in the reaction conditions of 50 mM potassium HEPES, 10 mM NaCl, pH 8.0, with 1 mM DTT for 20 h. Amino acid analysis was done as described above and in “Experimental Procedures.” Reactions were replicated twice. B. *C. elegans* PRMT-7 enzyme (2  $\mu$ g) was reacted with 12.5  $\mu$ M of various synthetic peptides (pSmD3, pRpl3, pR1, Histone H3 (1–7) and RGR-1),



at the conditions described in A. Reactions were single replicates. The reactions in the top panels for pSmD3 and pRpl3 are the same panels used in Fig. 2B right column.

Author Manuscript

Author Manuscript

Author Manuscript

Author Manuscript

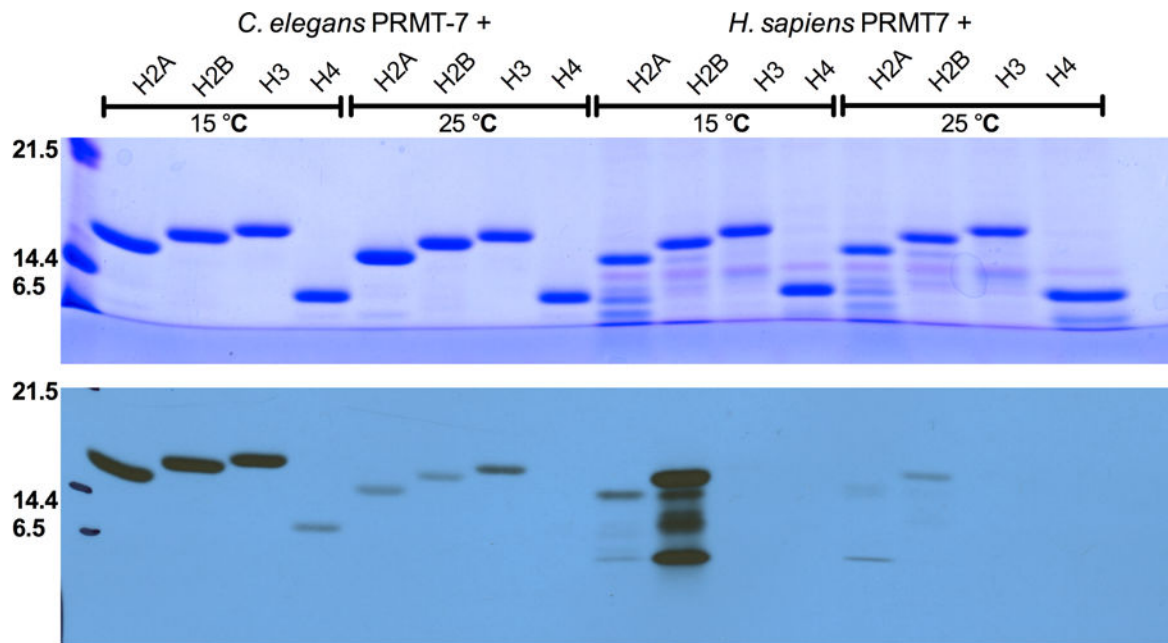


**Figure 6. *C. elegans* PRMT-7 has a distinct substrate specificity than the mammalian ortholog for mammalian histones**

Reactions consisting of 5  $\mu\text{g}$  of substrate (recombinant human histones from New England BioLabs (H2A: M2502S; H2B: M2505S; H3.3: M2507S; H4: M2504S) were reacted with 2  $\mu\text{g}$  of *C. elegans* GST-PRMT-7 or human GST-PRMT7 at 15 °C or 25 °C as described in “Experimental Procedures”. Reactions were stopped by the addition of sample loading buffer and polypeptides separated as described in “Experimental Procedures”. The dried gel was then exposed to autoradiography film for 3 d at  $-80$  °C. Molecular weight positions are shown from approximately 2  $\mu\text{g}$  of unstained SDS-PAGE broad range marker as in Fig. 3. The results shown here were replicated three times for *C. elegans* PRMT-7 and two times for human PRMT7. Radiolabeled bands migrating more rapidly than histone H2B in the lane with human PRMT7 appear to be proteolytic fragments.

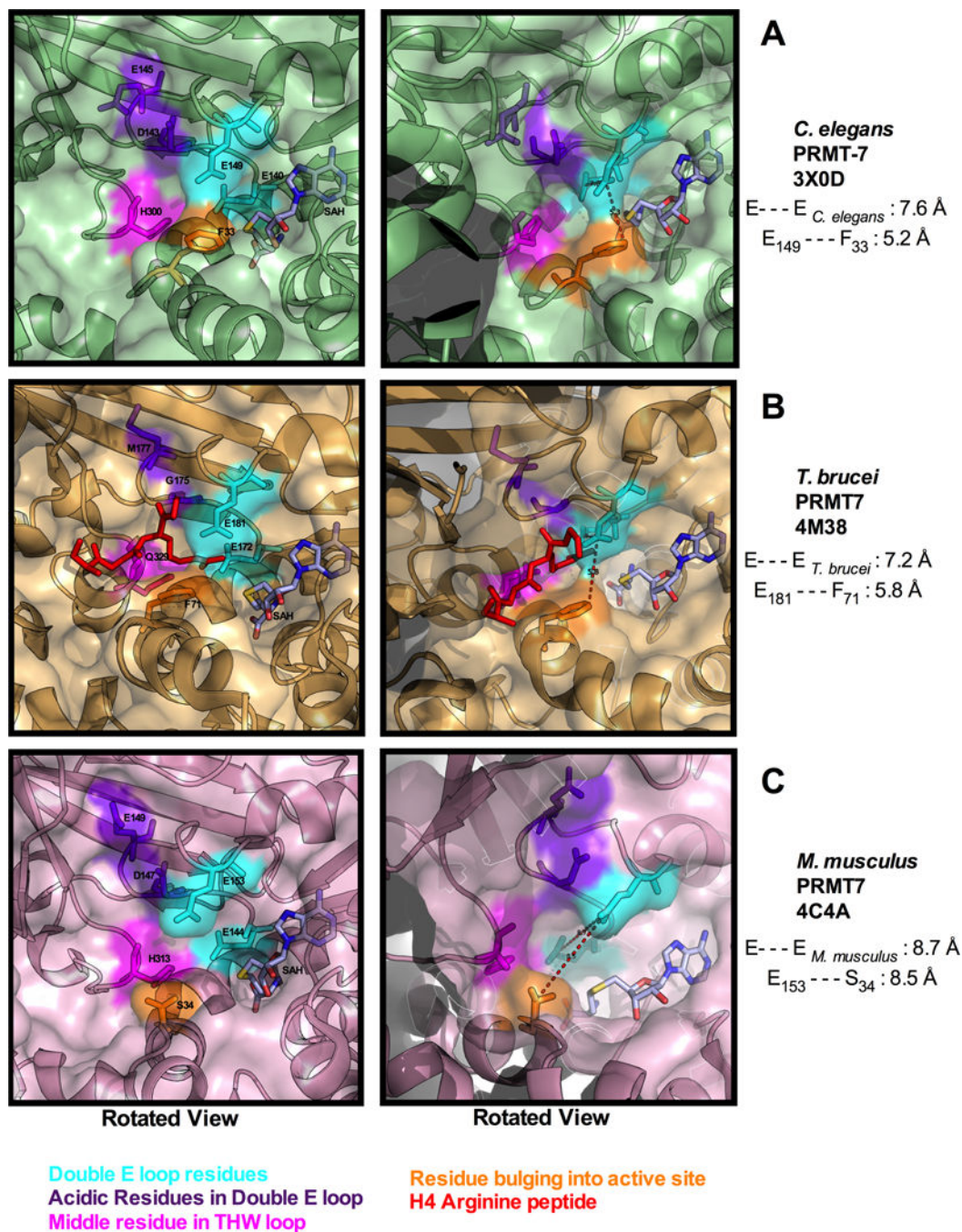


**Figure 7. Active site architecture of *C. elegans*, trypanosome, and mammalian PRMT7s**

A. Pymol surface and cartoon representation of the active site of *C. elegans* PRMT-7 (3X0D,<sup>24</sup>). Flanking glutamate double E loop residues are highlighted in cyan (E140, E149), internal loop acidic residues in purple (D143, E145), and a THW loop residue in magenta (H300). The residue highlighted in orange (F33) protrudes from a helix to form a cavity with E149. The distance from the side chain carboxyl carbon of E140 to the side chain carboxyl carbon of E149 is 7.6 Å, and distance from the side chain carboxyl carbon of E149 to the closest side chain carbon atom in F33 is 5.2 Å. *S*-Adenosylhomocysteine (SAH) is shown in

CPK coloring. B. Pymol surface and cartoon representation of the active site of *T. brucei* PRMT7 (4M38,<sup>20</sup>), highlighting residues corresponding to those shown in panel A. Flanking double E loop residues E172 and E181 are highlighted in cyan, G175 and M177 (residues corresponding to D143 and E145 residues in *C. elegans*) are highlighted in purple, and the Q329 THW loop residue is highlighted in magenta. The residue highlighted in orange (F71) corresponds to F33 in the *C. elegans* structure and also protrudes from a helix to form a cavity with E181. The distances between the flanking double E residues and E181-F71 are given as in panel A. The arginine-3 residue of the co-crystallized histone H4 peptide is modeled in red. C. Pymol surface and cartoon representation of active site of *M. musculus* PRMT7 (4C4A,<sup>25</sup>), highlighting residues corresponding to those shown in panels A and B. The distances between the flanking double E residues and E153-S34 are given as in panels A and B. We note that the S34 side chain oxygen is shown in two conformations.

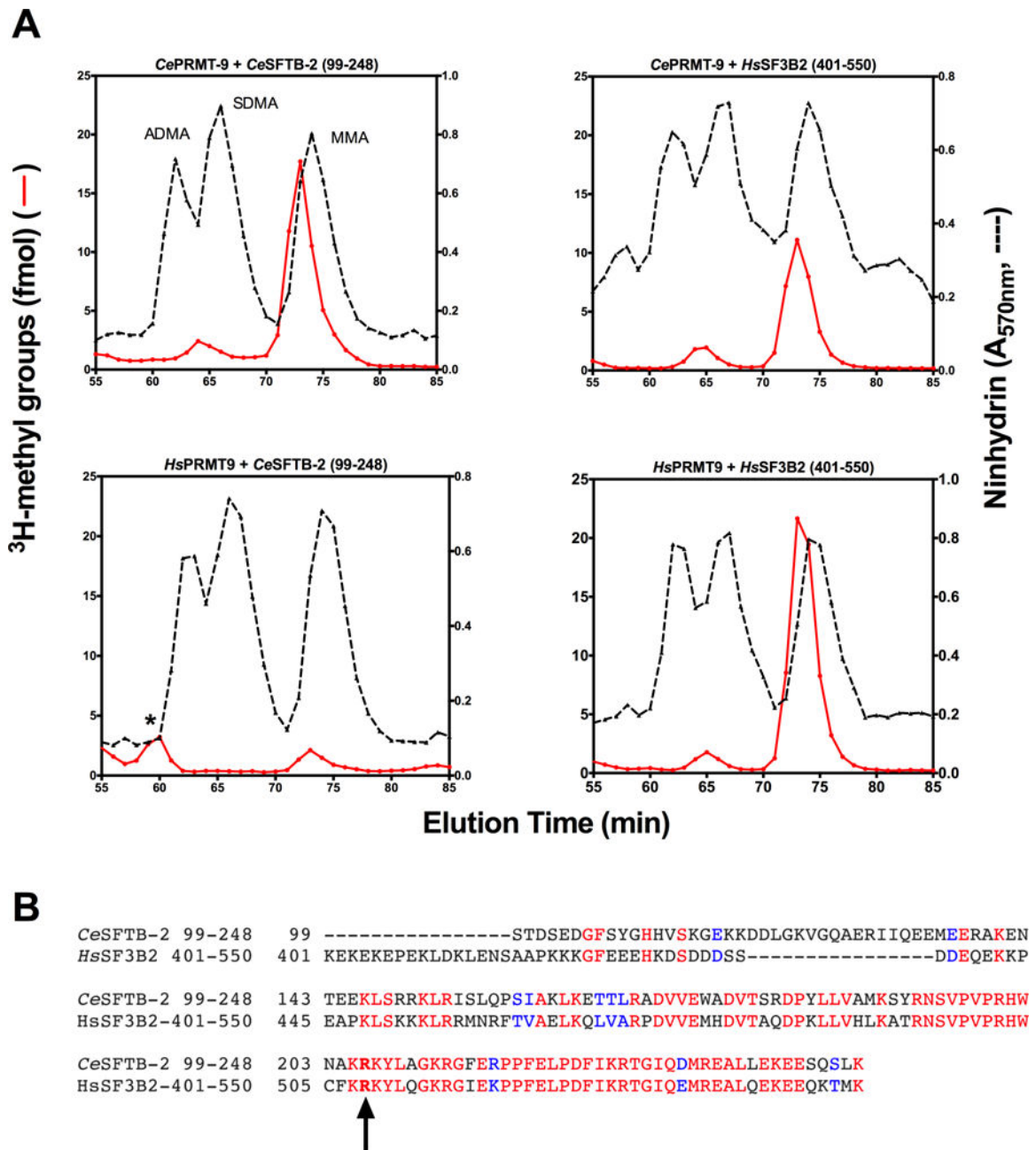


**Figure 8. *C. elegans* PRMT-9 symmetrically dimethylates SFTB-2, the *C. elegans* ortholog of the mammalian SF3B2**

A. Amino acid analysis was done as in Fig. 2 on methylation reactions consisting of 5  $\mu$ g of substrate (*C. elegans* GST-tagged SFTB-2 fragment 99–248 or *H. sapiens* GST-tagged SF3B2 fragment 401–550) and approximately 2  $\mu$ g of enzyme (*C. elegans* GST-tagged PRMT-9 enzyme or *H. sapiens* GST-tagged PRMT9 enzyme) that were incubated for 20 h at 25 °C (nematode enzyme) or 37 °C (human enzyme) in a reaction buffer consisting of 50 mM potassium HEPES, 10 mM NaCl, pH 8.2, with a final concentration of 0.7  $\mu$ M [*methyl*-<sup>3</sup>H]AdoMet in a volume of 60  $\mu$ l. The reactions were quenched by the addition of final concentration 12.5% trichloroacetic acid and acid hydrolyzed as described in the

materials and methods. The asterisk indicates a radioactive peak eluting prior to the expected position of  $^3\text{H}$ -ADMA. The experiment was replicated twice. B. Sequence alignment of *C. elegans* SFTB-2 (UniProt ID: O16997) residues 99–248 and human SF3B2 (UniProt ID: Q13435, bottom). Red letters indicate identity and blue letters indicate similar amino acid properties. Bolded R and black arrow indicates methylation site for the enzyme.

Author Manuscript

Author Manuscript

Author Manuscript

Author Manuscript

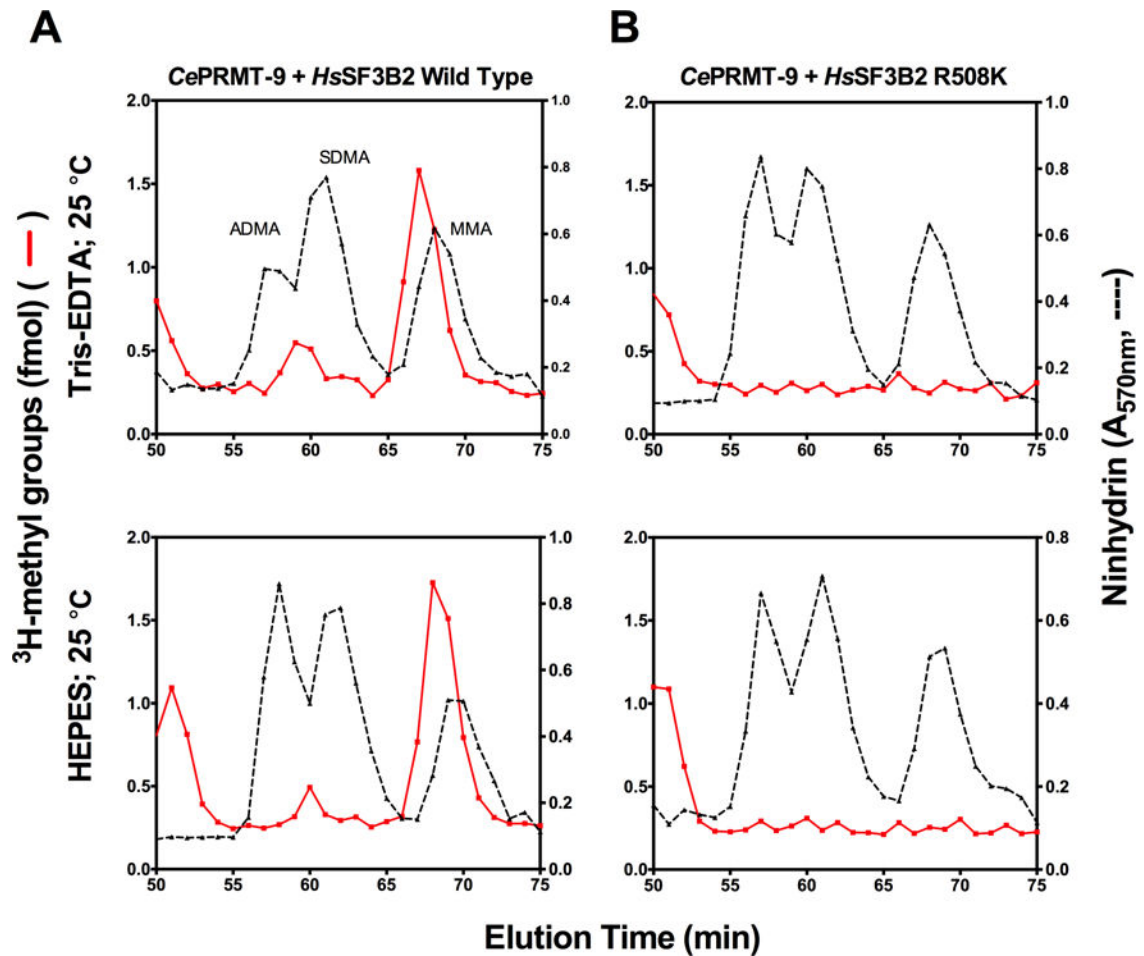


**Figure 9. *C. elegans* PRMT-9 methylates SF3B2 at the same R508 site that is methylated by the mammalian PRMT9 enzyme**

A. Amino acid analysis of methylation reaction consisting of 2  $\mu\text{g}$  of *C. elegans* GST-PRMT-9 enzyme with 5  $\mu\text{g}$  of human GST-SF3B2 (401–550) wild type at 25°C for 20 h in either 100 mM Tris-EDTA buffer pH 8.0 (top panel) and 50 mM potassium HEPES, 10 mM NaCl, pH 8.2 (bottom panel). Reactions were quenched by the addition of final concentration of 12.5% trichloroacetic acid and acid hydrolyzed as described above. Reactions were duplicated twice.

B. Methylation reactions of *C. elegans* PRMT-9 enzyme was reacted with human GST-SF3B2 (401–550) R508K mutant fragment, in the same reaction conditions described in part A at 25 °C for 20 h. Reactions were duplicated twice.

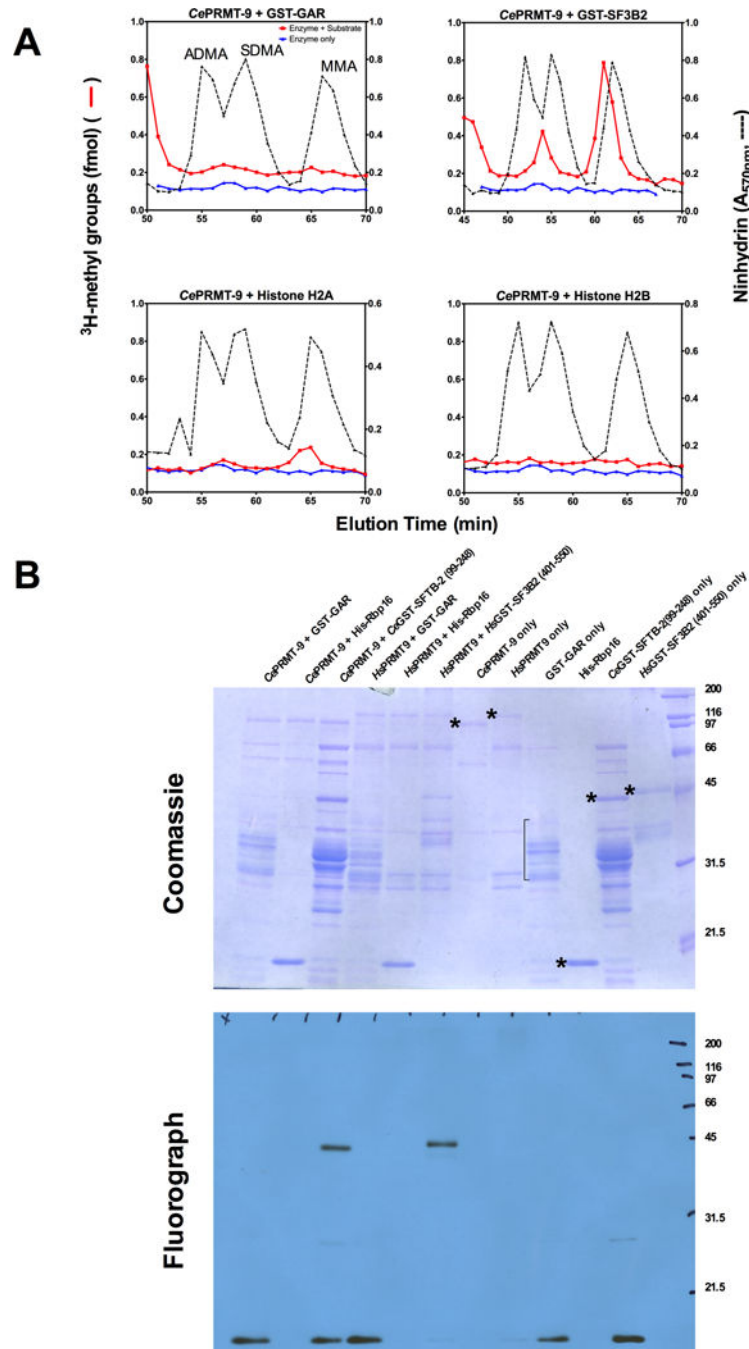


**Figure 10. Substrate specificity of *C. elegans* PRMT-9**

A. Methylation reactions for amino acid analysis were set up using  $2\ \mu\text{g}$  of *C. elegans* PRMT-9 with  $5\ \mu\text{g}$  of various substrates (GST-GAR, top left; GST-SF3B2 (401–550), top right; recombinant human histone H2A, bottom left; recombinant human histone H2B bottom right), in 100 mM Tris-EDTA buffer, pH 8.0, for 6 h at  $30\ ^\circ\text{C}$ , conditions defined in Takahashi et al.<sup>23</sup>. These reactions using these conditions were single replicates. B. *In vitro* methylation reactions consisting of  $2\ \mu\text{g}$  of *C. elegans* PRMT-9 or human PRMT9 enzyme were reacted with  $5\ \mu\text{g}$  of substrate (GST-GAR, His-Rbp16, or GST-SFTB-2 (*C. elegans*



fragment 99–248) or GST-SF3B2 (human fragment 401–550) for 20 h at 25 °C (*C. elegans*) or 37 °C (human) in 50 mM potassium HEPES, 10 mM NaCl, 1 mM DTT, pH 8.2 with 0.7  $\mu$ M [*methyl*-<sup>3</sup>H]AdoMet. Sample loading buffer was added to stop the reactions and polypeptides were separated using SDS-PAGE, using the same methods described in Fig. 3. The gel was then dried and exposed to film for 7 days at –80 °C. Coomassie stained gel is shown on top, and the fluorographic exposure is shown below. The molecular weight standards are shown as described in Fig. 3. This experiment was replicated independently using amino acid analysis.

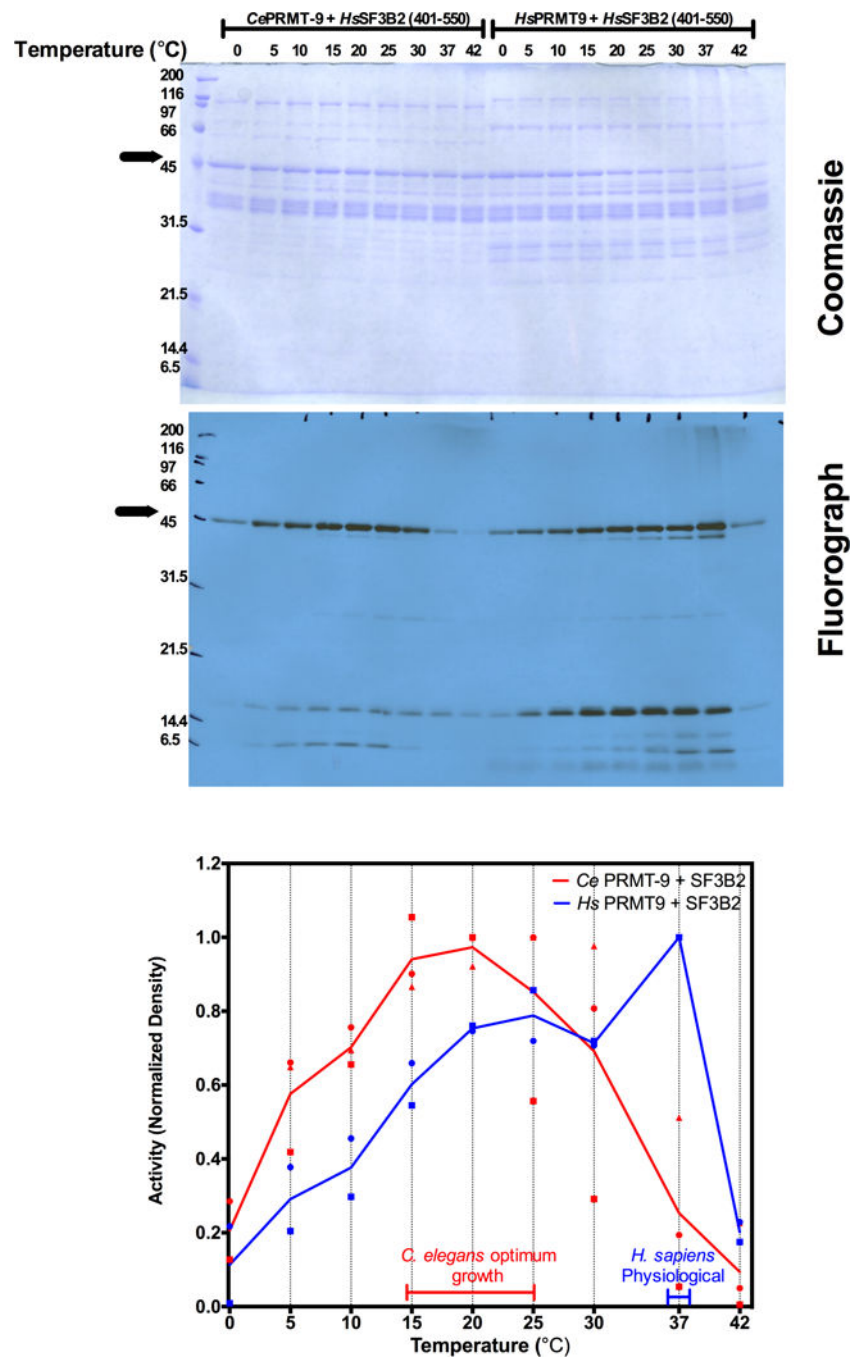


**Figure 11. Temperature dependence of *C. elegans* PRMT-9**

Methylation reactions consisting of 5  $\mu\text{g}$  of substrate (*H. sapiens* GST-tagged SF3B2 fragment 401–550) were reacted with 2  $\mu\text{g}$  of enzyme (both *C. elegans* and *H. sapiens* PRMT9 enzymes) at the various temperatures indicated for 20 h at the reaction conditions of 50 mM potassium HEPES, 10 mM NaCl, pH 8.2 with 0.7  $\mu\text{M}$  [*methyl*- $^3\text{H}$ ]AdoMet in a final reaction volume of 60  $\mu\text{l}$ . Reactions were quenched by the addition of sample loading buffer and proteins were separated using SDS-PAGE using the same methods described in Fig. 3. The gel was dried and exposed to autoradiography film for 21 d at  $-80^\circ\text{C}$ . Coomassie gel

(top panel) and fluorograph (lower panel) are shown. Molecular weight positions are shown from approximately 2  $\mu\text{g}$  of unstained SDS-PAGE broad range marker as described in Figure 3. This experiment was replicated independently and a third replicate using the *C. elegans* PRMT-9 enzyme was done. The bottom panel indicates the densitometry of the bands comparing methylation activity of the *C. elegans* enzyme to the human enzyme. Densitometry was done using ImageJ software on the scanned images of the films and quantified similarly to Fig. 3 (*C. elegans*, red symbols; human, blue symbols). A solid line is drawn for the average of the normalized values of the replicates. The optimal growth temperatures for *C. elegans*<sup>31</sup> and humans are indicated.

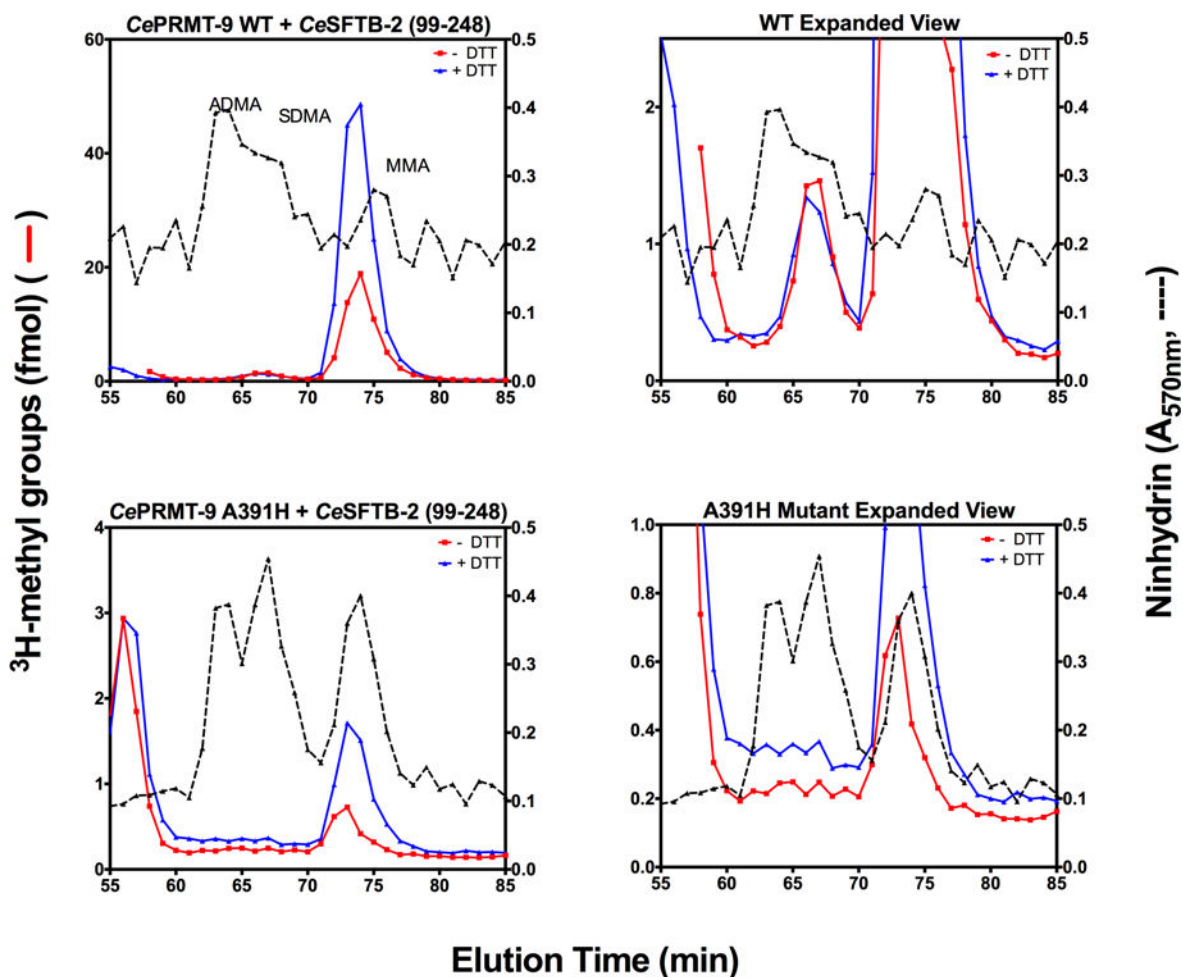


**Figure 12. *C. elegans* PRMT-9 THW loop residues are important for conferring SDMA specificity and a small DTT effect**

*C. elegans* PRMT-9 enzyme (2  $\mu$ g) wild type (top row) or THW loop mutant A391H (bottom row) was reacted with approximately 5  $\mu$ g of *C. elegans* SFTB-2 for 20 h at 25 °C in the reaction buffer containing 50 mM potassium HEPES, 10 mM NaCl, pH 8.0, with (blue line) or without 1 mM DTT (red line), as indicated. Mutation of the THW loop residue A391 to the conserved histidine residue abolishes the SDMA activity, producing only MMA, consistent with previous work with the human enzyme PRMT9 C431H mutant<sup>22</sup>. These reactions were single replicates.